



## Transthyretin mutagenesis: impact on amyloidogenesis and disease

Zaida L. Almeida, Daniela C. Vaz & Rui M. M. Brito

**To cite this article:** Zaida L. Almeida, Daniela C. Vaz & Rui M. M. Brito (07 Jun 2024): Transthyretin mutagenesis: impact on amyloidogenesis and disease, *Critical Reviews in Clinical Laboratory Sciences*, DOI: [10.1080/10408363.2024.2350379](https://doi.org/10.1080/10408363.2024.2350379)

**To link to this article:** <https://doi.org/10.1080/10408363.2024.2350379>




© 2024 The Author(s). Published by Informa UK Limited, trading as Taylor & Francis Group



Published online: 07 Jun 2024.



[Submit your article to this journal](#) 



[View related articles](#) 



[View Crossmark data](#) 

## Transthyretin mutagenesis: impact on amyloidogenesis and disease

Zaida L. Almeida<sup>a</sup>, Daniela C. Vaz<sup>a,b,c</sup> and Rui M. M. Brito<sup>a</sup>

<sup>a</sup>Chemistry Department and Coimbra Chemistry Centre - Institute of Molecular Sciences (CQC-IMS), University of Coimbra, Coimbra, Portugal; <sup>b</sup>School of Health Sciences, Polytechnic Institute of Leiria, Leiria, Portugal; <sup>c</sup>LSRE-LCM – Leiria, Portugal & ALiCE – Associate Laboratory in Chemical Engineering, University of Porto, Porto, Portugal

### ABSTRACT

Transthyretin (TTR), a homotetrameric protein found in plasma, cerebrospinal fluid, and the eye, plays a pivotal role in the onset of several amyloid diseases with high morbidity and mortality. Protein aggregation and fibril formation by wild-type TTR and its natural more amyloidogenic variants are hallmarks of ATTRwt and ATTRv amyloidosis, respectively. The formation of soluble amyloid aggregates and the accumulation of insoluble amyloid fibrils and deposits in multiple tissues can lead to organ dysfunction and cell death. The most frequent manifestations of ATTR are polyneuropathies and cardiomyopathies. However, clinical manifestations such as carpal tunnel syndrome, leptomeningeal, and ocular amyloidosis, among several others may also occur. This review provides an up-to-date listing of all single amino-acid mutations in TTR known to date. Of approximately 220 single-point mutations, 93% are considered pathogenic. Aspartic acid is the residue mutated with the highest frequency, whereas tryptophan is highly conserved. “Hot spot” mutation regions are mainly assigned to  $\beta$ -strands B, C, and D. This manuscript also reviews the protein aggregation models that have been proposed for TTR amyloid fibril formation and the transient conformational states that convert native TTR into aggregation-prone molecular species. Finally, it compiles the various *in vitro* TTR aggregation protocols currently in use for research and drug development purposes. In short, this article reviews and discusses TTR mutagenesis and amyloidogenesis, and their implications in disease onset.

**Abbreviations:** AD: Alzheimer’s disease; ATTR: TTR amyloidosis; ATTRwt: wild-type TTR amyloidosis; ATTRv: hereditary TTR amyloidosis; ATTRv-PN: hereditary TTR amyloidosis with polyneuropathy; ATTRv-CM: hereditary TTR amyloidosis with cardiomyopathy; ATTRv-LM: hereditary leptomeningeal TTR amyloidosis; ATTRv-OC: hereditary ocular TTR amyloidosis; BBB: blood–brain barrier; CNS: central nervous system; CR: Congo red; CSF: cerebrospinal fluid; DCVJ: (9-(2,2-dicyanovinyl) julolidine); DMSO: dimethyl sulfoxide; EDTA: ethylenediaminetetraacetic acid; HSA: human serum albumin; hATTR: hereditary TTR amyloidosis; HTS: high throughput screening; hTTR: human TTR; LDL: low-density lipoprotein; PBS: phosphate-buffered saline; PDB: Protein Data Bank; PNS: peripheral nervous system; RBP: retinol-binding protein; RPE: retinal pigment epithelium; SDS: sodium dodecyl sulfate; T3: triiodothyronine; T4: thyroxine; TBG: thyroxine-binding globulin; TFE: 2,2,2-trifluoroethanol; THAOS: Transthyretin Amyloidosis Outcomes Survey; THDPs: thyroid hormone distributor proteins; THs: thyroid hormones; ThT: thioflavin-T; TTR: transthyretin; wt: wild-type

### ARTICLE HISTORY

Received 12 March 2024

Revised 17 April 2024

Accepted 29 April 2024

### KEYWORDS

Amyloid; ATTR; aggregation; transthyretin (TTR); TTR variants

## 1. Introduction

Protein aggregation and amyloid formation contribute to several debilitating diseases collectively known as Amyloidosis [1]. To date, more than fifty amyloid diseases have been identified, including localized amyloidosis found in neurodegenerative conditions like Alzheimer’s and Parkinson’s diseases, and systemic amyloidosis such as transthyretin amyloidosis and lysozyme amyloidosis [1]. These pathologies result from

mutations, post-translational modifications, or partial proteolysis, and by abnormal folding or unfolding events affecting approximately fifty different peptides/proteins. These end up adopting non-native, misfolded conformations prone to aggregate into highly ordered soluble oligomers and insoluble fibrils with a characteristic cross- $\beta$  structure – the amyloid substance. Generally, amyloid diseases are not a consequence of the loss of function of the native protein but result

**CONTACT** Zaida L. Almeida  zalmeida@qui.uc.pt; Daniela C. Vaz  daniela.vaz@ipleiria.pt; Rui M. M. Brito  brito@ci.uc.pt  Chemistry Department and Coimbra Chemistry Centre - Institute of Molecular Sciences (CQC-IMS), University of Coimbra, 3004-504 Coimbra, Portugal.

© 2024 The Author(s). Published by Informa UK Limited, trading as Taylor & Francis Group

This is an Open Access article distributed under the terms of the Creative Commons Attribution License (<http://creativecommons.org/licenses/by/4.0/>), which permits unrestricted use, distribution, and reproduction in any medium, provided the original work is properly cited. The terms on which this article has been published allow the posting of the Accepted Manuscript in a repository by the author(s) or with their consent.

from the cytotoxic nature of the amyloid aggregates and/or the action of amyloid fibrils on inter-cellular communication and tissue physiology. Although most amyloids are found extracellularly, amyloid-like deposits are also found inside cells [1].

Transthyretin amyloid disorders include sporadic age-related wild-type TTR amyloidosis (ATTRwt), hereditary TTR amyloidosis polyneuropathy (ATTRv-PN), hereditary TTR amyloidosis cardiomyopathy (ATTRv-CM), hereditary leptomeningeal TTR amyloidosis (ATTRv-LM) and hereditary ocular TTR amyloidosis (ATTRv-OC). Although some of the ATTR clinical manifestations have unmet medical needs, in the last decade several disease-modifying therapies have contributed to slowing down disease progression and, in some cases, have ameliorated disease symptoms. The continuing efforts to better understand the molecular mechanisms of disease progression and tissue specificity are critical for the rational development of new and improved therapies for the treatment of TTR amyloidoses.

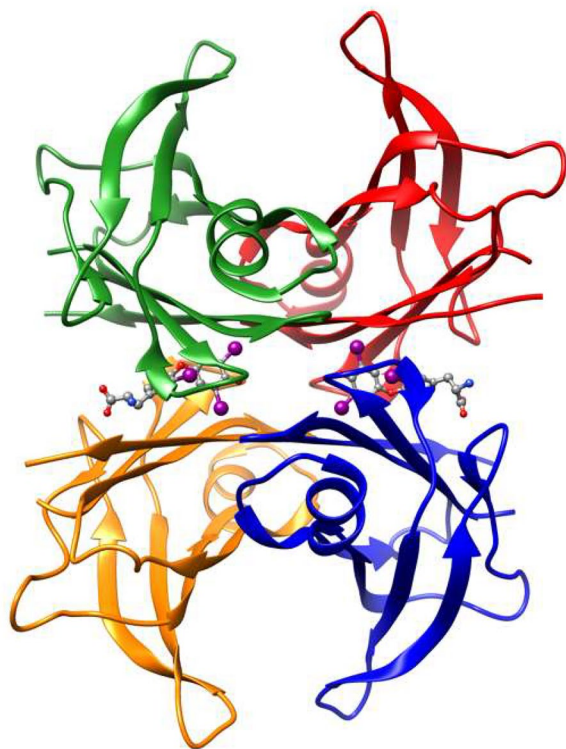


**Figure 1.** Three-dimensional structure representation of the native TTRwt homotetramer. The structure is composed of four identical subunits (each represented in a different color) forming a central channel able to accommodate two thyroxine (T4) molecules (depicted in a ball-and-stick representation). The image was produced with UCSF Chimera [19] and coordinates of the crystallographic structure of human TTRwt in a complex with T4 (PDB code: 1ICT).

## 2. Transthyretin structure and function

### 2.1. From prealbumin to transthyretin (TTR)

In 1942, a new protein was identified and named “prealbumin” due to its electrophoretic mobility just ahead of serum albumin, both in plasma [2] and cerebrospinal fluid (CSF) [3]. Later, in 1958, prealbumin was found to bind thyroid hormones, being therefore renamed as “thyroxine-binding prealbumin” [4]. In 1969, additional studies showed that thyroxine-binding prealbumin could also bind the retinol-binding protein (RBP) [5]. The International Union of Biochemists then coined the name “transthyretin” (TTR) in 1981 [6] due to its ability to transport thyroid hormones (THs), especially thyroxine (T4), as well as retinol (vitamin A) in association with RBP.

### 2.2. Transthyretin biosynthesis, tissue concentration, and metabolism

TTR is a globular homotetrameric protein, with a total molecular mass of approximately 55 kDa, consisting of four monomers with an identical sequence of 127 amino acids (Figure 1). In humans, TTR is mainly found in plasma [7], CSF [8–11], and the eye [12–16]. Serum TTR accounts for nearly 90% of TTR in the human organism and is secreted by the liver to concentrations (as tetramers) varying from 0.17 to 0.42 mg/mL (3.1 to 7.6  $\mu$ M) [7].

In CSF, TTR has been reported as one of the most abundant proteins, along with serum albumin, prostaglandin-D synthase, and immunoglobulins [8]. Since serum TTR does not cross the blood–brain barrier (BBB) to any significant extent, a different source of production apart from the liver must account for the protein in the CSF at a concentration range between 0.005 to 0.02 mg/mL (0.09 to 0.36  $\mu$ M) [11]. Indeed, TTR synthesis has been reported to occur in the epithelial cells of the choroid plexus [9,10]. Expression of the TTR gene was also found in Schwann cells, dorsal root ganglia [17], and cortical and hippocampal neurons in response to amyloid- $\beta$  (A $\beta$ )-induced stress, in patients with Alzheimer’s disease (AD) [18].

TTR is also found in the eye [12–14]. Since the Bruch membrane that encircles more than half of the eye is a barrier to protein crossing, intraocular TTR synthesis is required and has been reported in the retinal pigment epithelium (RPE), the pigmented epithelium of the ciliary body, corneal endothelium, and the optic nerve fiber layer of the retina [12–14]. The concentration of TTR in the aqueous humor is approximately

1.3  $\mu\text{g}/\text{mL}$  (0.024  $\mu\text{M}$ ) [15], while in the vitreous humor is nearly 18  $\mu\text{g}/\text{mL}$  (0.327  $\mu\text{M}$ ) [16].

TTR biosynthesis has also been described in several other tissues to a smaller extent, namely in the heart, skeletal muscle, spleen [20], visceral yolk sac endoderm [21], trophoblasts of placenta [22], gastric ghrelin cells [23], pineal gland [24], meninges [25] and pancreatic  $\alpha$ -cells [26,27].

Furthermore, TTR serum levels are slightly higher in adulthood than in childhood, higher in men than in women, and start to decline after 40 years of age [28]. The half-life of serum TTR is approximately 2 to 3 days in humans [29,30]. The main sites for TTR degradation are the liver (36–38%), muscle (12–15%), and skin (8–10%), along with other minor sites, such as the kidney, adipose tissue, testicles, and gastrointestinal tract (1–8%), and other tissues in less than 1% [31]. Serum levels of TTR are routinely measured as an indicator of health status, since TTR is a typical negative acute-phase serum protein [32]. TTR serum levels are reduced in conditions such as trauma, surgery, inflammation, bacterial infection, protein malnutrition, coronary artery disease, depression, Alzheimer's disease, gestational diabetes mellitus, and Down's syndrome [33–39].

### 2.3. Transport of thyroid hormones and retinol

The term "transthyretin" describes the dual physiological role of the protein in the transport of thyroid hormones (THs) and retinol [6]. Although binding with higher affinity to T4 (thyroxine or 3,5,3',5'-tetraiodo-L-thyronine) than to T3 (triiodothyronine or 3,5,3'-triiodo-L-thyronine), TTR is able to transport both THs. Thyroid hormones show a common structure consisting of a hydrophobic thyronine nucleus, which accounts for their poor solubility in water, a hydrophilic hydroxyl group attached to the phenolic ring, and three iodine atoms in positions 3, 5, and 3' in the case of T3, and four iodine atoms in positions 3, 5, 3' and 5' in the case of T4. In human plasma, 99.97% of T4 and 99.70% of T3 are bound to TH distributor proteins (THDPs), namely human serum albumin (HSA), TTR, and thyroxine-binding globulin (TBG) [40,41]. THDPs circulate at different concentrations and show distinct dissociation constants ( $K_d$ ) and affinity for THs [42]. TBG, a monomeric 54 kDa protein with a single binding site, has the highest affinity for T4 and T3 with  $K_d$  of 0.1 and 2 nM, respectively. Due to its high binding affinity and despite its low plasma concentration of 0.015 mg/mL, TBG binds approximately 75% of both T4 and T3 in plasma. TTR has two binding sites with the highest affinity binding event with  $K_d$  values of 14 nM for T4 and 57 nM for T3 [43]. Binding to a second thyronine

molecule occurs with a significantly lower affinity, through negative cooperativity [44]. Present in plasma at a concentration between 0.17 and 0.42 mg/mL, TTR binds nearly 15% of T4 and less than 5% of T3. Conversely, HSA, a monomeric 66.5 kDa protein with various binding sites, has the lowest affinity for THs with dissociation constants of 1.4  $\mu\text{M}$  for T4 and 100  $\mu\text{M}$  for T3. Due to its low binding affinity and despite its high serum concentration of 35–50 mg/mL, HSA binds less than 5% of T4 and less than 20% of T3. Additionally, a small fraction of THs is also distributed in the bloodstream by lipoproteins, including ApoB100, *via* interaction with its cell surface receptor, i.e. the low-density lipoprotein (LDL) receptor [45,46]. TTR is the only TH transport protein synthesized in the choroid plexus and, therefore, plays a significant role in transporting THs in the CSF and distributing THs in the brain [47].

The transport of retinol is mediated by RBP [48]. RBP circulates in the plasma bound to TTR. Both apo- (without) and holo- (with retinol) RBPs form the RBP-TTR complex with a stoichiometry of 2:1, with approximately 97 kDa [49,50]. However, the  $K_d$  of holo-RBP with TTR is significantly lower than with apo-RBP [51], which is consistent with a retinol delivery mechanism where the stable holo-RBP-TTR complex is retained in the plasma, while the unbound apo-RBP, with lower molecular weight (21 kDa) is cleared by glomerular filtration [52]. The binding sites for RBP are located at the surface of TTR, and each TTR molecule has four RBP-binding sites, two in each dimer. However, due to steric hindrance, only two RBP molecules bind simultaneously to TTR [49]. RBP and TTR contribute 21 amino acids each to the protein-protein recognition interface, with most of these residues located in the C-terminal regions of the two proteins [50]. Affinity measurements of TTR to RBP estimate a  $K_d$  of 150 to 190 nM for the first RBP molecule and 35  $\mu\text{M}$  for the second RBP, indicating negative cooperativity [53,54]. Ratios of RBP:TTR in plasma are around 0.3 in healthy individuals [55,56] indicating that most of the circulating TTR remains free of RBP.

## 3. Transthyretin amyloidoses

### 3.1. Transthyretin amyloid diseases, symptoms, and geographic distribution

Transthyretin amyloidosis (ATTR) is manifested in sporadic and hereditary forms: wild-type TTR amyloidosis (ATTRwt) and hereditary TTR amyloidosis (ATTRv). In the case of hereditary TTR amyloidosis, polyneuropathy (ATTRv-PN) and cardiomyopathy (ATTRv-CM) are the most common clinical manifestations. While ATTRv-PN

mostly affects the peripheral nervous system (PNS), ATTRv-CM mainly targets the heart. Additionally, other forms of ATTRv such as leptomeningeal amyloidosis (ATTRv-LM) and ocular amyloidosis (ATTRv-OC) affect the central nervous system (CNS) and the vitreous body of the eye, respectively. Nonetheless, some patients simultaneously exhibit multiple symptoms associated with distinct manifestations of ATTRv. That is the case of hereditary TTR amyloidosis polyneuropathy with muscle, vitreous, leptomeningeal, and cardiac involvement [57–59].

In contrast, ATTRwt, formerly known as senile systemic amyloidosis, is a non-hereditary age-related systemic amyloidosis caused by TTRwt. The main features of each type of ATTR are described in Table 1.

In an effort to better understand the natural history and phenotypic heterogeneity of TTR amyloidosis, as well as improving diagnosis and treatment, the Transthyretin Amyloidosis Outcomes Survey (THAOS), the largest global, longitudinal, observational survey of patients with ATTR amyloidosis (inherited and wild-type), as well as of asymptomatic TTR gene carriers, has been established and formally ongoing since 2007 [60].

### 3.2. Transthyretin amyloidogenic and non-amyloidogenic variants

Hereditary TTR amyloidoses (ATTRv) are fatal diseases triggered by TTR variants that have been classified as “amyloidogenic” TTR mutants. ATTRv amyloidoses are autosomal-dominant diseases, where only one amyloidogenic variant TTR allele is required to develop pathology. Most affected individuals are heterozygous for a pathogenic mutation and express both normal (TTRwt) and variant TTR (TTRv), but some homozygous patients have also been identified [86,87]. The majority of the mutations result from a single nucleotide substitution in the TTR gene [88]. Transthyretin has been identified as one of the most mutated human proteins leading to the development of amyloid diseases [89].

In 1952, the pioneering work of Corino de Andrade produced the first medical reports on the diagnosis of ATTRVal30Met amyloidosis among a group of families, from the north of Portugal [90], conducing to the discovery of other foci in Japan (1968) and Sweden (1976) [91, 92]. Until two decades ago, ATTRv-PN was thought to be an endemic disease restricted to those areas, but today is known to occur worldwide.

The human TTR gene is localized in chromosome 18 at position 12.1 (18q12.1) [93], spanning approximately 6.9kb (GenBank accession number: NG\_009490.1, and Gene ID: 7276). The TTR gene is divided into four exons

and three introns. Exon 1 encodes 23 amino acid residues, that is translated into 20 residues of a signal peptide and the first three residues of the mature protein. Exon 2 codes for amino acid residues 4 to 47, exon 3 for residues 48 to 92, and exon 4 for residues 93 to 127 [94]. Hence, the amino acid numbering used throughout this manuscript to identify the various mutations in the protein sequence refers to the 127 residues that compose the mature TTR monomer (e.g.: Val30Met or V30M). Nonetheless, another counting system that includes the 20-amino acid peptide signal (labeled as p.) is also used elsewhere (e.g.: p.Val50Met or p.V50M).

Figure 2 lists the 216 point mutations identified in the TTR gene so far, by depicting their position in the 127 amino acid polypeptide chain of the TTR monomer [80,95–119]. Figure 2 includes all TTR mutations (amyloidogenic and non-amyloidogenic) reported in the open access page “Mutations in Hereditary Amyloidosis” (amyloidosismutations.com) [95], in the Human Genetic Mutation database (hgmd.cf.ac.uk) ([118]), in the ClinVar public archive of reports of human genetic variants (ncbi.nlm.nih.gov/clinvar) [119], along with other TTR mutations that have been documented in the literature through scientific papers and reports available at PubMed Central (pubmed.com). Commonly identified variants are well documented and have proper information on their clinical phenotype and natural history. However, regarding rare variants, it is difficult to obtain information on their amyloidogenic potential and clinical significance due to a lack of family history, reduced penetrance, and other factors. Most mutations result in single amino acid substitutions distributed across the polypeptide chain, except for the Val122\_del deletion mutation [120], the Met13\_dup and Glu51-Ser52\_dup duplication mutations [121,122], and the synonymous mutations Ala108Ala and Thr119Thr [123]. Double mutations have also been reported over time. Table 2 lists some of these TTR double mutations found in ATTRv patients.

A 7-residue length “window analysis” was employed here to scan the more than 200 TTR variants identified, as applied previously by other authors in 1996 to less than 50 TTR mutations [130]. This 7-window “view” helps to highlight “hot spot” regions, that would otherwise be masked when using the simple “mutations per residue” view (also shown in Figure 3A by the solid grey graph). A sliding window of 7-residues in length was moved from the N-terminus to the C-terminus in steps of one residue. The total number of mutations found in each window was plotted against the number of the midpoint-residue of each interval (Figure 3A). All variants were treated independently so that multiple

**Table 1.** Summary of human transthyretin-associated amyloidoses.

TTR Amyloidosis	Main organs and systems affected		Main symptoms	Observations	Age of onset and survival from onset	Geographic distribution	Most common TTR* variants
Wild-type TTR amyloidosis (ATTRwt)	Heart		Progressive breathlessness, right-sided heart failure, including lower extremity edema, elevated jugular venous pressure, hepatomegaly, ascites, anginal chest pain, palpitations associated with paroxysmal atrial arrhythmias, cerebrovascular events secondary to intracardiac thrombus. Syncope and lightheadedness may result from hypotension due to poor cardiac reserve compounded by arrhythmia [61]. In addition to universal cardiac manifestations, the involvement of soft tissues leads to an increased incidence of bilateral carpal tunnel syndrome, spinal stenosis, or spontaneous biceps tendon rupture [62].	Historically, ATTRwt was considered a rare condition predominantly affecting elderly subjects and mostly found at postmortem examination. This observation derived from low awareness of the disease, fragmented knowledge, and regular misdiagnosis due to phenotypic heterogeneity and overlap with other conditions [63]. ATTRwt is estimated to affect more than 25% of people over the age of 80, and 37% of people over the age of 95 [64]. However, the real number of affected individuals is currently unknown. Major insights into disease epidemiology revealed ATTRwt in 13% of patients older than 60 years hospitalized for heart failure with preserved ejection fraction [65], in 5% of patients with hypertrophic cardiomyopathy, and in 16% of patients with 'paradoxical' low-flow low-gradient aortic stenosis [66]. Cardiomyopathy due to ATTRwt is likely under-recognized since clinical diagnosis depends upon the appropriate interpretation of echocardiography or cardiac magnetic imaging. Moreover, with newer techniques, such as longitudinal strain imaging, T1 mapping on cardiac magnetic resonance imaging, and cardiac scintigraphy, the diagnosis of ATTRwt no longer requires tissue biopsies [67]. Particularly, there are some patients diagnosed with ATTRwt as early as the age of 34 and 47 [68,69]. Although peripheral and/or autonomic neuropathy are uncommon in ATTRwt, neuropathy can be seen in up to 10% of patients [70].	Strong male prevalence affects patients over 60 years old. Less than 5 years survival from onset of heart failure.	Worldwide	wt
Hereditary TTR amyloidosis with polyneuropathy (ATTR-PN)	Peripheral nervous system  Autonomic nervous system  Kidney  Gastrointestinal system  Carpus Thyroid Heart, CNS and eye		Peripheral sensory-motor neuropathy, axonal, fiber length-dependent, symmetric, and relentlessly progressive in distal to proximal direction.  Autonomic neuropathy, orthostatic hypotension, urinary tract infections, sexual dysfunction, sweating abnormalities.  Nephropathy, proteinuria, albuminuria, mild azotemia renal failure.  Nausea and vomiting, early satiety, diarrhea, severe constipation, alternating episodes of diarrhea and constipation, unintentional weight loss.  Carpal-tunnel syndrome. Hypothyroidism. See cardiomyopathy, leptomeningeal TTR amyloidosis, and ocular TTR amyloidosis symptoms, respectively.	ATTRVal30Met early-onset (age <50 years) involves 3 stages: Stage 1 - Progressive sensory polyneuropathy leading to walking difficulties without assistance; Stage 2 - Sensory motor polyneuropathy needing walking assistance; Stage 3 - Wheelchair-bound patients or bedridden until death. ATTRVal30Met and ATTRv-PN late-onset (age >50 years) caused by other mutations: faster disease development with earlier gait disability and earlier need for walking assistance until the patient is wheelchair-bound, resulting in faster progression of the sensory-motor neuropathy. In 2018, 10,186 patients (5,526 to 38,468 patients) with ATTRv-PN were globally estimated [71]. ATTRv-PN incidence is likely to increase with the increased awareness of the condition among clinicians and the wider use of genetic testing, particularly in non-endemic regions. TTRVal30Met is the most common mutant identified among smaller disease clusters and scattered families worldwide [72]. Studies have shown that the same genotype may be associated with different ages of onset, epidemiological, genetic, epigenetic, pathological, and clinical features, as in the case of Portuguese, Japanese, and Swedish patients with the Val30Met mutation [73].	The age of onset is around 30 years for the early onset disease caused by the Val30Met mutation, but depending on the TTR variant may vary up to 90 years old. Near 12 years survival in early-onset patients carrying the Val30Met mutation. Approximately 7 years of survival in late-onset patients carrying Val30Met TTR or other variants.	Worldwide, but endemic to certain areas of Portugal, Sweden, Japan, Brazil, Cyprus, and Majorca.	Val30Met Gly47Glu Thr60Ala Ser77Tyr Glu89Gln

(Continued)

Table 1. Continued.

Main organs and systems affected		Main symptoms	Observations	Age of onset and survival from onset	Geographic distribution	Most common TTR* variants
Hereditary TTR amyloidosis with cardiomyopathy (ATTRv-CM)	Heart	Same as in wild-type TTR amyloidosis (ATTRwt)	The major cause of death in ATTRv-CM is refractory heart failure due to cardiac infiltration of amyloid deposits into the extracellular matrix. The Val122Ile mutation is commonly associated with ATTRv-CM and is found almost exclusively among African descendants, showing a prevalence of 3.4% in the African American population [74], approximately 5% in the West African population [75] and nearly 8.5% in the Afro-Caribbean population [76]. Patients with Val122Ile TTR show later onset and have a higher degree of cardiac infiltration than patients carrying other TTR mutations [77]. Worldwide prevalence of ATTRv-CM is still uncertain, although it is estimated that 100,000-150,000 individuals of African American ethnicity can be at risk of developing the disease in the U.S.A. [78]. Historically, appropriate diagnosis of ATTRv-CM required the detection of amyloid fibrils by endomyocardial tissue biopsy. However, more recently technetium scintigraphy imaging has proven to be a reliable method of diagnosis for this amyloidosis without the need for invasive techniques [79]. CNS and ocular diseases can either occur separately or combined (oculoleptomeningeal amyloidosis), or even with the involvement of other organs [59]. ATTRv-LM is characterized by amyloid deposition preferentially in the pia-arachnoid and leptomeningeal vessels. In most cases it is believed that the source of the variant TTR in ATTRv-LM is not the liver, but the choroid plexus [81]. Ocular manifestations are present amongst 10% of patients with ATTRv-PN and usually occur later during the course of the disease or after hepatic transplantation [82]. TTR mutations Arg34Gly, Lys35Thr, Trp41Leu, Tyr69His and Gly83Arg affect only the eye [83]. Authors believe that the source of the TTR variant causing ocular amyloidosis is not the liver, but the retinal pigment epithelium [84].	Variable onset, depending on mutation (30-80years), but most ATTRv-CM patients show late-onset cardiac amyloidosis (after 60years old). The life expectancy of an ATTRv-CM patient is variable, depending on genetic mutation, but normally 2 to 5 years after the onset of symptoms.	Worldwide, but prevalent among African American, Afro-Caribbean, West African, British, Danish, and Italian populations.	Thr60Ala Leu111Met Val122Ile Ile68Leu
	Central nervous system (CNS)	Progressive dementia, headaches, dizziness, vomiting, hallucinations, ataxia, stroke-like episodes, episodes of focal neurological deficits, epilepsy, cerebral hemorrhage and infarction, hydrocephalus, spastic paralysis, and convulsions [58,80].				
Hereditary ocular TTR amyloidosis (ATTRv-OC)	Eye	Vitreous opacities, chronic open-angle glaucoma, abnormal conjunctival vessels, keratoconjunctivitis sicca, loss of corneal sensitivity and neurotrophic corneal ulcers, anterior capsule opacity of the lens, retinal vascular changes, pupillary light-near dissociation, irregular pupil, optic neuropathy [82].				
				The mean age of onset is approximately 45years. Depending on the TTR variant, survival expectancies vary from 5 to 18 years.  The mean time of survival after ATTRv-PN onset is estimated to be around 10 years and the mean time of occurrence of ATTRv-OC after orthotopic liver transplantation is approximately 5 years [85].	Rare	Asp18Gly Ala25Thr Val30Met Val30Gly Tyr69His Tyr114Cys  Val30Met Phe33Ile Ala36Pro Glu54Lys Phe64Ser Ile84Ser Tyr114Cys

\*Amino acid numbering according to the 127-residue sequence of the mature protein, without the 20-residue signal peptide.

	Pro2Leu	Thr3Met	Gly4Asp Gly4Ser	Gly6Ser					Cys10Arg	
1	2	3	4	5	6	7	8	9	10	11
Gly	Pro	Thr	Gly	Thr	Gly	Glu	Ser	Lys	Cys	Pro
G	P	T	G	T	G	E	S	K	C	P

Leu12Met						Asp18Glu <sup>(2)</sup>		Val20Ala		
Leu12Val	Met13 <sub>dnp</sub>					Asp18Asn		Val20Leu		
Leu12Pro	Met13Ile	Val14Leu				Asp18Gly	Ala19Asp	Val20Ile	Arg21Gln	Gly22Asp
12	13	14	15	16	17	18	19	20	21	22
Leu	Met	Val	Lys	Val	Leu	Asp	Ala	Val	Arg	Gly
L	M	V	K	V	L	D	A	V	R	G

**β-strand A**

Ser23Arg		Ala25Thr		Val28Ser		Val30Leu <sup>(2)</sup>		Phe33Cys	
Ser23Asn	Pro24Ser	Ala25Ser	Ile26Val	Asn27Ser	Val28Met	Val30Ala	His31Pro	Val32Gly	Arg34Thr
Ser	Pro	Ala	Ile	Asn	Val	Val30Ala	His31Asn	Val32Ala	Arg34Ser
S	P	A	I	N	V	A	V	H	R

**β-strand B**

Ala36Pro	Ala37Asp	Asp38Val	Asp39Tyr	Thr40Asn		Glu42Asp		Phe44Leu	Ala45Val		Gly47Val
Ala36Asp	Ala37Thr	Asp38Ala	Asp39Val	Thr40Asn	Trp41Leu	Glu42Gly	Pro43Ser	Phe44Ser	Ala45Thr		Gly47Glu
Ala	Ala	Asp	Asp	Thr	Trp	Glu	Pro	Phe	Ala	Ser	Gly
A	A	D	D	T	W	E	P	F	A	S	G

**β-strand C**

Thr49Ala	Ser50Gly					Glu54Ser					
Thr49Ser	Ser50Asn	Glu51Ser52 <sub>dnp</sub>	Gly53Ala		Glu54Gly	Leu55Pro		Thr59Ala			
Thr49Ile	Ser50Ile	Glu51Ala	Ser52Tyr	Gly53Glu	Glu54Leu	Leu55Arg	His56Tyr	Leu58His	Thr59Lys	Thr60Ile	
Thr49Pro	Ser50Arg <sup>(2)</sup>	Glu51Gly	Ser52Pro	Gly53Arg	Glu54Lys	Leu55Gln	His56Arg	Gly57Arg	Leu58Arg	Thr59Arg	Thr60Ala
49	50	51	52	53	54	55	56	57	58	59	60
Thr	Ser	Glu	Ser	Gly	Glu	Leu	His	Gly	Leu	Thr	Thr
T	S	E	S	G	E	L	H	G	L	T	T

**β-strand D**

Glu61Ala								Tyr69Cys	Lys70Asn <sup>(2)</sup>	
Glu61Gly	Glu62Asp		Phe64Leu <sup>(2)</sup>			Gly67Glu		Tyr69Ile	Lys70Gln	
Glu61Lys	Glu62Lys		Phe64Val		Glu66Asp	Gly67Arg	Ile68Leu <sup>(2)</sup>	Tyr69His	Lys70Glu	Val71Ala
61	62	63	64	65	66	67	68	69	70	71
Glu	Glu	Glu	Phe	Val	Glu	Gly	Ile	Tyr	Lys	Val
E	E	E	F	V	E	G	I	Y	K	V

**β-strand E**

Asp74His	Thr75Ile		Ser77Tyr				Ala81Ser		Ile84Leu	
Asp	Thr	Lys	Ser	Tyr	Lys80Arg	Ala81Thr	Leu82Pro		Ile84Asn	
D	T	K	S	Y	W	A	L		Ile84Ser	

**α-helix**

His88Arg	Glu89Asp								Ala97Asp	
His88Gln	Glu89Val	His90Asp			Val94Gly			Thr96Arg	Ala97Gly	Asp99Asn
His	Glu	His	Ala	Glu	Val	Phe	Thr	Ala	Ala	Asn
H	E	H	A	E	V	F	T	A	N	D

**β-strand F**

Gly101Asp		Arg103Cys				Ile107Thr					Tyr114Ser
Gly101Ser	Pro102Arg	Arg103His	Arg104His		Thr106Asn	Ile107Met	Ala108Val	Ala109Val			Tyr114His
Gly	Pro	Arg	Arg	Tyr	Thr	Ile	Ala	Ala	Leu	Leu	Pro
G	P	R	R	Y	T	I	A	A	L	L	P

**β-strand G**

									Val122Leu	
	Tyr116Ser		Thr118Ile	Thr119Thr	Ala120Thr				Val122Ala	
	Tyr116Val	Ser117Thr	Thr118Met	Thr119Met	Ala120Ser				Val122Ile	
115	116	117	118	119	120	121	122	123	124	125
Ser	Tyr	Ser	Thr	Thr	Ala	Val	Val	Thr	Asn	Pro
S	Y	S	T	T	A	V	V	T	N	P

**β-strand H**

**Figure 2.** Amino-acid sequence derived from the human 127-residue TTR mature protein showing the position of 216 mutations formally identified. Non-amyloidogenic mutations are displayed in green, while aggressive amyloidogenic mutations are colored in red. Duplication mutations are in orange, and a deletion mutation is in blue. Elements of secondary structure are displayed according to the TTRwt crystallographic structure, at 1.15 Å resolution (PDB code: 8AWI), with the β-strands highlighted in light blue, the α-helix in light red, and loops and turns in black.

variants at a single site were considered separately when determining the number of variants within the scanning window. A random distribution of TTR mutations would be expected to produce an approximately linear horizontal plot along the polypeptide chain, with 11.7 residues at each window position with a standard

deviation of  $\pm 5.1$ . However, the observed distribution is quite different from a random distribution.

According to [Figure 3A](#), there are two major peaks of mutation frequency, one centered at residue 52 and another centered around residues 33-36, that also define two major mutation "hot spot" regions, Region 1 and 2, formed by residues 44-59 and 26-43, respectively. Region 1 computed 27 substitutions in the 7-residue window, with a height of 3.0 standard deviations above the mean. Both of these regions map the mutation "hot spot" zone of TTR, mainly assigned to  $\beta$ -strand D and CD and DE loops in the case of Region 1, and to  $\beta$ -strand B, which is parallel and hydrogen bonded to  $\beta$ -strand C, the second half of  $\beta$ -strand C and the BC loop, for Region 2. Five more subsidiary regions can also be observed in [Figure 3A](#): Region 3, composed of residues 60-76 assigned to the DE loop,  $\beta$ -strand E, and to the  $\alpha$ -helix; Region 4, represented by residues 97-112 located in  $\beta$ -strand G, GH, and FG loops; Region 5, formed by residues 77-96 which corresponds to  $\beta$ -strand F and the  $\alpha$ F loop; Region 6, with residues 113-125, corresponding to  $\beta$ -strand H and the C-terminus; and Region 7, allocated to residues 14-25 of the AB loop. The protein regions involved in dimer-dimer interactions include loops AB and GH which are part of Regions 4 and 7, and the segments involved in monomer-monomer

**Table 2.** TTR double mutations found in ATTRv patients and their protein sequence localization, according to the 127-residue numbering of the mature protein. These may occur in the same or different gene alleles.

Double mutations	Localization	References
Gly6Ser/Ala19Asp	N-terminus/AB loop	[122,124-129]
Gly6Ser/Val30Met	N-terminus/ $\beta$ -strand B	
Gly6Ser/Phe33Ile	N-terminus/ $\beta$ -strand B	
Gly6Ser/Ala45Asp	N-terminus/ $\beta$ -strand C	
Gly6Ser/Thr49Ile	N-terminus/CD loop	
Gly6Ser/Ser77Tyr	N-terminus/ $\alpha$ -helix	
Gly6Ser/Tyr114Cys	N-terminus/GH loop	
Gly6Ser/Thr119Met	N-terminus/ $\beta$ -strand H	
Gly6Ser/Val122Ala	N-terminus/ $\beta$ -strand H	
Val30Met/His90Asn	$\beta$ -strand B/ $\beta$ -strand F	
Val30Met/Arg104His	$\beta$ -strand B/ $\beta$ -strand G	
Val30Met/Thr119Met	$\beta$ -strand B/ $\beta$ -strand H	
Val30Met/Val122Ile	$\beta$ -strand B/ $\beta$ -strand H	
Phe33Ile/Thr49Gly	$\beta$ -strand B/CD loop	
Glu42Gly/His90Asn	$\beta$ -strand C/ $\beta$ -strand F	
Thr59Lys/Arg104His	DE loop/ $\beta$ -strand G	
His90Asn/Thr119Met	$\beta$ -strand F/ $\beta$ -strand H	
Tyr116His/Val122Ile	$\beta$ -strand H/ $\beta$ -strand H	

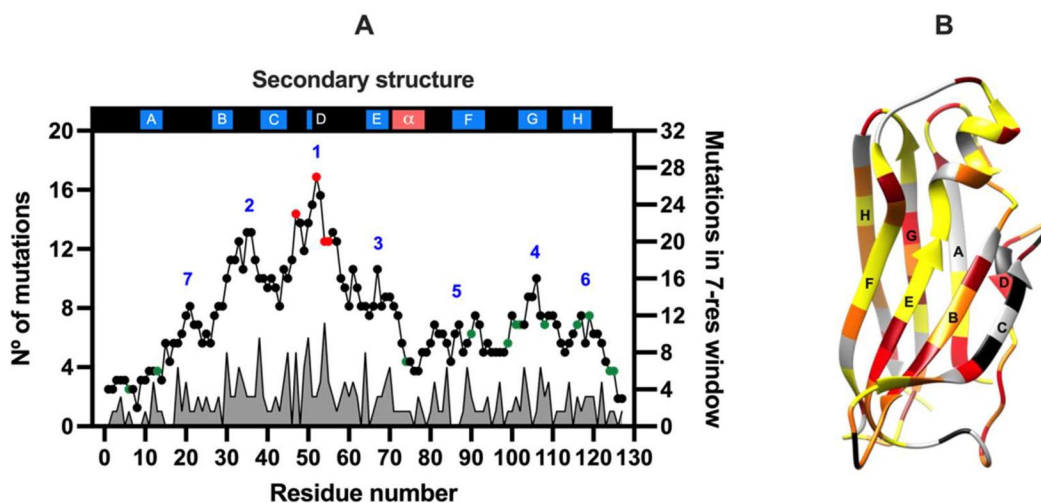


**Figure 3.** Naturally occurring mutation "hot spot" zones of the 127-amino acid human transthyretin subunit mature sequence. **(A)** Plot of the TTR mutation frequency along the polypeptide chain. A graphical record of the total number of mutations per amino acid is shown in solid grey. In addition, a graph representing a sliding window of 7-residues in length that moves along the sequence plotting the total number of mutations (solid circles and black trace) of each interval against the midpoint residue of the interval is also shown [130]. Most aggressive amyloidogenic (red circles) and non-amyloidogenic (green circles) variants are identified. Regions with a high frequency of mutations are numbered from 1 to 7 (in blue). The duplication mutations (Met13\_dup and Glu51-Ser52\_dup) and the deletion mutation (Val122\_del) were not considered in the analysis. Elements of secondary structure are displayed at the top of the figure:  $\beta$ -strands (blue) and  $\alpha$ -helix (light red). **(B)** Three-dimensional structure representation of the TTR subunit backbone, with the elements of secondary structure ( $\beta$ -strands A to H) colored according to the number of mutations known per sequence position: "no substitutions" (grey); one (yellow); two (orange); three (red); four (dark red); and five or more (black). The image was produced with UCSF Chimera [19], using the coordinates of the TTRwt crystallographic structure at 1.15 Å resolution (PDB code: 8AWI).

**Table 3.** Regions of TTR high mutation frequency, and their characterization concerning residue number, structure localization, exon localization, and number of mutations per region along the 127-amino acid mature sequence of human TTR. Duplication mutations (Met13\_dup and Glu51-Ser52\_dup) and the deletion mutation (Val122\_del) were not considered in the analysis.

Region	Residues	Localization	Exon	N° of mutations
1	44-59	$\beta$ -strand D CD loop	2, 3	48
2	26-43	part of the DE loop $\beta$ -strands B and C BC loop	2	39
3	60-76	part of the DE loop $\beta$ -strand E $\alpha$ -helix	3	29
4	97-112	part of the FG loop $\beta$ -strand G GH loop	4	26
5	77-96	$\alpha$ F loop $\beta$ -strand F	3, 4	26
6	113-125	$\beta$ -strand H C-terminal	4	18
7	14-25	AB loop	2	16

interactions like  $\beta$ -strands H and F, located in Regions 5 and 6, can be seen in [Figure 3A](#). Most of the mutations found in Region 1 were the first mutations to be identified in the TTR gene [131]. [Table 3](#) summarizes the Regions identified, their amino-acid residues, localization in the polypeptide chain, exons involved, and number of mutations.

Another interesting observation, that can also be inferred from [Figure 3A](#), is that the mutations classified as the most aggressive amyloidogenic TTR mutations (causing disease with an early age of onset, with multiple organ involvement and severe impairment), namely Gly47Arg [132], Ser52Pro [133], Glu54Gly [134], Glu54Lys [135] and Leu55Pro [136] are all located in the Region 1 mutation “hot spot” (residues 44-59); whereas the TTR non-amyloidogenic mutations [96,99] (Gly6Ser, Met13Ile, Asp74His, His90Asn, Asp99Asn, Gly101Ser, Gly101Asp, Pro102Arg, Arg104His, Ala108Ala, Ala108Val, Ala109Thr, Tyr116Val, Thr119Thr, Thr119Met, and Pro125Ser) are preferentially located in Regions 4 and 6 (residues 97 to 125). In addition, some parts of the polypeptide chain present a low frequency of mutations, as is the case of the N-terminus (11 residues and 6 mutations), and the C-terminus (5 residues and 3 mutations). Exon 3 (residue 48 to 92) is the most mutated exon with 87 mutations, followed by exon 2 (residue 4 to 47) with 77 mutations, exon 4 (residue 93 to 127) with 50 mutations, and exon 1 (residue 1 to 3) with 2 mutations. The regions with the highest and the lowest mutation frequencies stand out when the 3D backbone structure of the TTR subunit is color-mapped ([Figure 3B](#)), revealing major “hot spots” at  $\beta$ -strands B, C, and D, as shown in red, dark red, and black.

A complete understanding of the effects of each point mutation on the overall structure and stability of the TTR monomers and tetramer is essential to unravel sequence–structure relationships. The group of mutations found to either stabilize or destabilize the protein varies according to the nature of the substituted amino acid. Some mutations affect crucial interactions within the protein, which in turn lead to misfolding and aggregation (amyloidogenic variants), while others can be innocuous (non-amyloidogenic or protective variants).

According to [Figure 4](#), aspartic acid is the most frequently replaced/mutated residue of the protein sequence, followed by arginine, isoleucine, phenylalanine, and alanine. TTRwt contains 5 aspartic acids (Asp) in its sequence (Asp18, Asp38, Asp39, Asp74, and Asp99) which have all been associated with one or more mutations per residue (Asp18Asn, Asp18Glu (2 $\times$ ), Asp18Gly, Asp38His, Asp38Tyr, Asp38Asn, Asp38Gly, Asp38Val, Asp38Ala, Asp39Tyr, Asp39Val, Asp74His, and Asp99Asn – 14 in total). In opposition, other residues show high conservation propensities, like tryptophan, asparagine, proline, and lysine. On the other hand, the residues that most frequently replaces the original residues present in TTRwt are serine, arginine, and alanine; a fact that directly correlates with the high number of RNA codons coding for these residues in the genetic code. Serine substitutes several different residues along the protein sequence and is present in 25 TTR mutants (Gly4Ser, Gly6Ser, Pro24Ser, Ala25Ser, Asn27Ser, Val28Ser, Arg34Ser, Pro43Ser, Phe44Ser, Ala45Ser, Thr49Ser, Glu54Ser, Phe64Ser, Ala81Ser, Ile84Ser, Ala91Ser, Ala97Ser, Gly101Ser, Arg103Ser, Ala109Ser, Tyr114Ser, Tyr116Ser, Ala120Ser, Asn124Ser, and Pro125Ser) which have largely been identified as amyloidogenic (exceptions are Gly6Ser, Gly101Ser, and Pro125Ser). Inversely, the residue which less frequently replace mutated residues is tryptophan (one single RNA codon), followed by phenylalanine, cysteine, and glutamine, with only two RNA codons available in the genetic code [137]. TTRwt contains 2 tryptophan residues (Trp) in its sequence (Trp41 and Trp79), but only one mutation associated with Trp41 has been identified (the amyloidogenic mutation Trp41Leu).

Additionally, even if all amyloidogenic, different pathogenic TTR mutations may produce different phenotypes, with different clinical manifestations and targeted organs, either leading to polyneuropathy, cardiomyopathy, vitreous opacities, carpal tunnel syndrome, CNS dysfunction, or leptomeningeal involvement. That is the case of residue in position 114, with 3 mutations identified ([Figure 2](#)). While Tyr114Cys conduces to ATTRv-PN [138], Tyr114Ser causes ATTRv-CM [139],

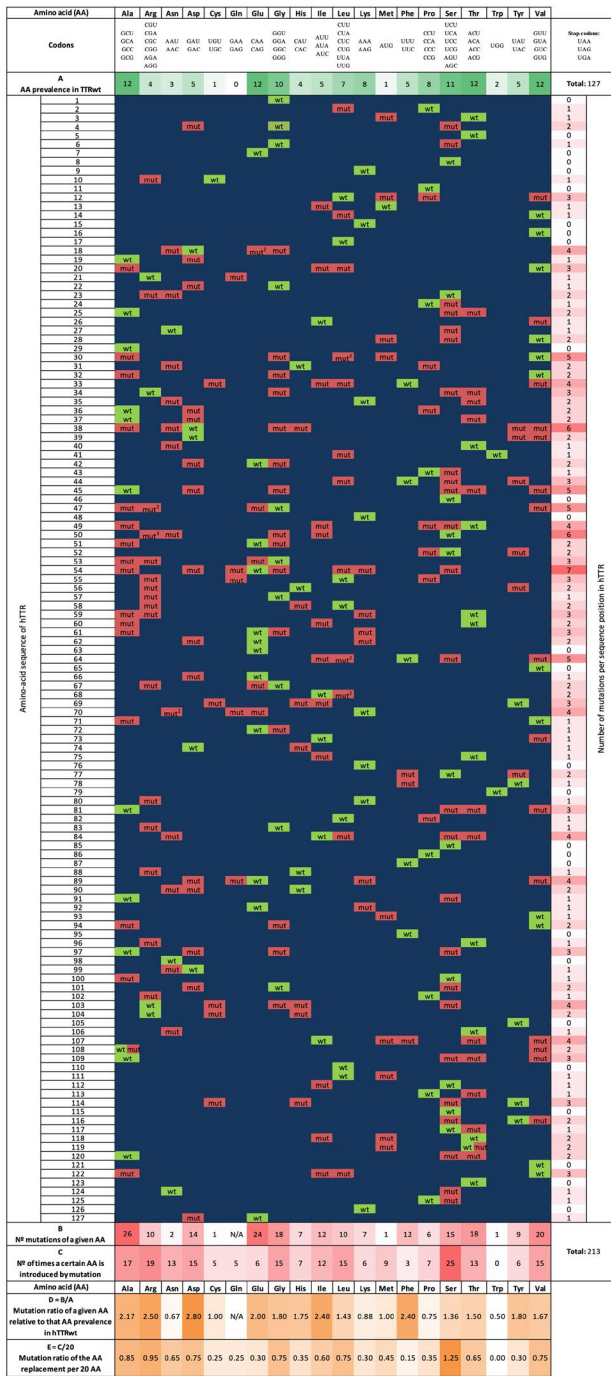


**Figure 4.** TTR mutation map. TTRwt residues are represented in green (wt) and mutations in red (mut). The scheme depicts the type of amino acid (AA), number and location of known naturally occurring mutations in the mature 127-residue sequence of hTTR, as well as: i) AA prevalence in hTTRwt (A); ii) the number of mutations a given AA suffers (B) (e.g. Asp is the amino acid that suffers most mutations, in fact, all Asp residues in the sequence have suffered mutations); iii) number of times a certain AA is introduced by mutation (C) (e.g. Ser is the AA most often introduced by mutation, being involved in a total of 25 mutations, so far, mostly amyloidogenic); iv) respective mutation ratio relative to the prevalence of each AA in hTTRwt ( $D=B/A$ ); and v) mutation ratio of the introduction of a given AA per 20 AA ( $E=C/20$ ). The duplication mutations (Met13\_dup and Glu51-Ser52\_dup) and the deletion mutation (Val122\_del) were not included in the diagram. N/A – non-applicable.

and Tyr114His is implicated in hereditary carpal tunnel syndrome ATTRv [140]. On the other hand, in the case of residue in position 45 all five known amyloidogenic variants specifically target the heart: Ala45Val, Ala45Ser, Ala45Thr, Ala45Gly, and Ala45Asp [111,141–144]. Similarly, mutation of residue in position 47 also leads to a unique phenotype, in this case ATTRv-PN, as observed in Gly47Arg, Gly47Ala, Gly47Glu, and Gly47Val [145–148].

Mutations of the TTR gene have already been associated with more than 200 pathogenic variants (Figure 2), and the reason why different mutations produce distinct clinical manifestations and different onset ages is still under investigation. Even when multiple symptoms are present in patients carrying the same mutation, clinical phenotypes do not always coincide, and the same mutation may be associated with different symptoms, their severity, and age of onset, even within the same kindred [149]. A clear example is the distinct pathological phenotype observed in Val30Met TTR carriers, with three main endemic foci in Portugal, Sweden, and Japan. Val30Met Portuguese and Japanese kindreds generally experience disease early onsets (below age 50, normally 30-40), severe disease, and high disease penetrance [150,151], while Val30Met Swedish families often present disease late onsets (above age 50, usually 60), intermediate disease severity, and low disease penetrance [152]. Nevertheless, beyond these endemic foci, other unrelated Val30Met TTR carriers have also been identified worldwide, where late-onset cases have found to be more prevalent and widely spread [153]. This clinical heterogeneity seems to be strongly correlated with the amyloid fibril composition found in the amyloid deposits of ATTRv patients. The early onset of the disease is associated with deposits containing only full-length TTR (type B fibrils), whereas the late onset of the disease is related to deposits with a mixture of full-length TTR and large amounts of C-terminal TTR fragments (type A fibrils) [154, 155] and composed by a combination of amyloidogenic TTRv and TTRwt [156]. Another example of heterogeneous disease onset is the case of the Thr60Ala TTR variant that has been associated with early and late disease onsets (23 and 70years old women, respectively) [157,158], causing simultaneously severe restrictive ATTRv-CM and ATTRv-PN. These observations indicate that the basis of the amyloid phenotype expression is not only due to a certain disease-triggering mutation, but also the amyloid fibril composition and type and eventually other genetic and environmental factors [73,159–161]. Recent studies showed that non-coding regions and the variation of the mutations in the TTR gene may also influence the phenotypic heterogeneity of ATTRv [162–169].

**Table 4.** Transthyretin aggregation models proposed over the years and their limitations.

Amyloidogenic intermediate	Aggregation model description	TTR* variant	Experimental conditions	Limitations of the aggregation model	References
Tetramer	<p>TTRVal30Met crystal structure at pH 5.7 showed that substituting Val at position 30 is transferred to the protein core to Cys10, which holds the single thiol group of the TTR subunit, which becomes slightly more exposed. The TTRVal30Met is in a near-native state. Molecular dynamics and experimental assays have shown that it is possible to model a linear aggregate of inter-tetrameric association, with each tetramer linked to the next by a pair of disulfide bonds involving Cys10 residues (two cysteines from one tetramer are linked by disulfide bridges to two cysteines in another TTR tetramer, thus making a long chain of tetramers). Formation of these disulfide bonds involves a small number of slightly short molecular contacts between native tetramers, most of which are altered in TTRVal30Met.</p> <p>The triple mutation leads to structural changes in residues 34–63, including the BC loop and <math>\beta</math>-strand C, CD loop, and <math>\beta</math>-strand D, leaving the tetramer distorted but intact, suggesting that this structure displays a more amyloidogenic-like behavior. TTR molecules aggregate until the formation of a triplet of tetramers. Two triplets fit together creating a starting point or nucleus for an amyloid fibril, which may continue to grow by adding more molecules in the form of tetramers, doublets, triplets, etc. Another possibility is that the first triplet continues to grow until a certain point when it gets intertwined with a second identical helix.</p> <p>Pressure-induced denaturation of TTR results in an altered tetrameric state with amyloidogenic properties highly sensitive to protein concentration, at 37 °C. After a cycle of compression-decompression at 1 °C, the main species are tetramers, with a small population of monomers. This non-native tetramer conformation is less stable under pressure, and on decompression forms aggregates under mild acidic conditions (pH 5.0–5.5). Pressure-treated samples bound thioflavin-T and Congo red dyes, a property of amyloid fibrils.</p>	Val30Met	TTR crystals were grown under conditions of 43% w/v saturated ammonium sulfate, 200mM sodium citrate, pH 5.7.	There is a TTR variant where Cys10 is replaced by Arg (TTRCys10Arg). This variant is known to form amyloid fibrils and, consequently, ATTRv-PN. Ionic strength, pH, and TTR concentrations used for the preparation of crystals were not physiologic.	[195]
	<p>The triple mutation leads to structural changes in residues 34–63, including the BC loop and <math>\beta</math>-strand C, CD loop, and <math>\beta</math>-strand D, leaving the tetramer distorted but intact, suggesting that this structure displays a more amyloidogenic-like behavior. TTR molecules aggregate until the formation of a triplet of tetramers. Two triplets fit together creating a starting point or nucleus for an amyloid fibril, which may continue to grow by adding more molecules in the form of tetramers, doublets, triplets, etc. Another possibility is that the first triplet continues to grow until a certain point when it gets intertwined with a second identical helix.</p> <p>Pressure-induced denaturation of TTR results in an altered tetrameric state with amyloidogenic properties highly sensitive to protein concentration, at 37 °C. After a cycle of compression-decompression at 1 °C, the main species are tetramers, with a small population of monomers. This non-native tetramer conformation is less stable under pressure, and on decompression forms aggregates under mild acidic conditions (pH 5.0–5.5). Pressure-treated samples bound thioflavin-T and Congo red dyes, a property of amyloid fibrils.</p>	Gly53Ser/Glu54Asp/Leu55Ser	At room temperature, crystals of an engineered TTR mutant at 3 mg/mL (54.5 $\mu$ M) in 50 mM Tris, pH 7.5, mixed with 40%–42% polyethylene glycol 5000 monomethyl ether, 100 mM sodium citrate, pH 5.5, 100 mM ammonium sulfate.	Neither the protofibrils nor the fibrils showed the $\beta$ -crossed structure characteristic of amyloid structures. Use of an engineered TTR mutant. Temperature, ionic strength and TTR concentrations used for the preparation of crystals were not physiologic.	[196]
	<p>Pressure-induced denaturation of TTR results in an altered tetrameric state with amyloidogenic properties highly sensitive to protein concentration, at 37 °C. After a cycle of compression-decompression at 1 °C, the main species are tetramers, with a small population of monomers. This non-native tetramer conformation is less stable under pressure, and on decompression forms aggregates under mild acidic conditions (pH 5.0–5.5). Pressure-treated samples bound thioflavin-T and Congo red dyes, a property of amyloid fibrils.</p>	wt	TTR solutions at 0.055 mg/mL (1 $\mu$ M) in 50 mM Bis-Tris HCl, 100 mM KCl, pH 5.6, and 50 mM Tris-HCl, 100 mM KCl, pH 7.5, subjected to high pressure (until 3,500 bar) at 1 °C and 37 °C.	Pressure used in the experiments was not physiologic. No evidence in other natural TTR variants.	[197]
Dimer	<p>Proteolytic cleavage is the initial step of TTR aggregation. Formation of TTR amyloid fibrils from four protofibrils with N-terminal truncated dimers as basic building blocks since dimers can no longer reassociate to tetramers. The protofibrils could be arranged around a hollow core to form one amyloid fibril to fit the TTR amyloid fibril model derived from image reconstruction of electron micrographs and X-ray fiber diffraction.</p> <p>TTRwt refolds to a native tetramer at low concentrations. The introduction of a single point mutation facilitates an off-pathway fold that generates dimeric species. At low temperature (4 °C), these dimeric species form a meta-stable fold mainly through entropic forces. An increase in temperature results in an increase in <math>\beta</math>-sheet structure and aggregation. The aggregates form mature amyloid fibrils after the appearance of protofibrils.</p> <p>TTR undergoes structural rearrangements to afford a dimeric intermediate. However, there is the possibility of assembly through a tetrameric intermediate, since the natural tetramer is essentially two copies of a dimer. The amyloidogenic intermediate with a native-like dimeric interface (enhanced edges) ultimately forms amyloid fibrils through additional subunit interactions. The aggregates bind Congo red and have morphologies typical of amyloid fibrils.</p>	Gly6Ser Cys10Arg Thr60Ala Ser77Tyr Thr119Met	Crystals of TTR variants at 10–20 mg/mL (181.8–363.6 $\mu$ M) grown in 100 mM citrate buffer, pH 5.5, at 23 °C precipitated with 1.5–3.0 M ammonium sulfate.	TTR proteolysis leads to the formation of several amyloidogenic fragments. However, analysis of amyloid deposits <i>in vivo</i> demonstrated not only TTR fragments but also full-length TTR. Temperature, ionic strength, pH, and TTR concentrations used for the preparation of crystals were not physiologic.	[198]
	<p>TTRwt refolds to a native tetramer at low concentrations. The introduction of a single point mutation facilitates an off-pathway fold that generates dimeric species. At low temperature (4 °C), these dimeric species form a meta-stable fold mainly through entropic forces. An increase in temperature results in an increase in <math>\beta</math>-sheet structure and aggregation. The aggregates form mature amyloid fibrils after the appearance of protofibrils.</p> <p>TTR undergoes structural rearrangements to afford a dimeric intermediate. However, there is the possibility of assembly through a tetrameric intermediate, since the natural tetramer is essentially two copies of a dimer. The amyloidogenic intermediate with a native-like dimeric interface (enhanced edges) ultimately forms amyloid fibrils through additional subunit interactions. The aggregates bind Congo red and have morphologies typical of amyloid fibrils.</p>	wt Val14Asn/Val16Glu Gly53Ser/Glu54Asp/Leu55Ser	TTR samples at 0.02–0.55 mg/mL (0.36–10 $\mu$ M) denatured in 20 mM phosphate buffer, 50 mM NaCl, pH 7.0 with 8 M urea or 8 M Gdn-HCl. Refolding studies performed in 20 mM phosphate buffer, 50 mM NaCl, pH 7.0 at 4 °C or 20 °C.	The temperature used in the experiments was not physiologic. Use of engineered TTR mutants. No evidence of other natural TTR variants.	[199]
	<p>TTRwt refolds to a native tetramer at low concentrations. The introduction of a single point mutation facilitates an off-pathway fold that generates dimeric species. At low temperature (4 °C), these dimeric species form a meta-stable fold mainly through entropic forces. An increase in temperature results in an increase in <math>\beta</math>-sheet structure and aggregation. The aggregates form mature amyloid fibrils after the appearance of protofibrils.</p> <p>TTR undergoes structural rearrangements to afford a dimeric intermediate. However, there is the possibility of assembly through a tetrameric intermediate, since the natural tetramer is essentially two copies of a dimer. The amyloidogenic intermediate with a native-like dimeric interface (enhanced edges) ultimately forms amyloid fibrils through additional subunit interactions. The aggregates bind Congo red and have morphologies typical of amyloid fibrils.</p>	Glu89Cys/Thr96Cys	Engineered TTR mutant at 1 mg/mL (18.2 $\mu$ M) subjected at pH 4.4, 37 °C.	pH and TTR concentrations used in the experiments were not physiologic. Use of an engineered TTR mutant. No evidence in other natural TTR variants.	[200]

(Continued)

Table 4. Continued.

Amyloidogenic intermediate	Aggregation model description	TTR* variant	Experimental conditions	Limitations of the aggregation model	References
Monomer	<p>Lysosomes use acidic denaturation and proteolysis for protein degradation and are a possible site for amyloid fibril formation <i>in vivo</i>. The acid denaturation pathway of TTR is characterized by several different intermediates having variable quaternary, tertiary, and secondary structures. TTR dissociates to monomers in a process that is dependent on both acidic pH and protein concentration, at 37°C. TTRwt remains as a tetramer from pH 7.0 to pH 5.0 and is incapable of amyloid fibril formation. The extent of amyloid fibril formation correlates with the amount of TTR monomers having an altered but defined non-native tertiary structure, over the pH range of 5.0-3.9, where the maximal amyloid fibril formation is at pH 4.4. Aggregates bind Congo red. Below pH 4.4, the monomeric TTRwt intermediate begins to adopt alternative conformations that are not amyloidogenic. Amyloidogenic variants exhibit similar acid denaturation pathways than TTRwt, with the exception that tetramer dissociation to the monomeric amyloidogenic intermediate occurs at a higher pH and to a much greater extent.</p> <p>Monomeric TTR intermediates undergo transient unfolding in some <math>\beta</math>-strands while retaining a stable <math>\beta</math>-sheet core, which could provide a starting point for amyloid fibril formation in TTRwt and its variants, at pH 4.5.</p> <p>At pH 2.0, TTR tetramers dissociate into denatured monomers. When adding 100 mM NaCl to denatured monomers, there is a change to an A-state or molten globule. In addition, these monomers present a denatured transformation of the compact deep globule type which has the ability to aggregate over time.</p> <p>Amyloid fibrils isolated from vitreous humor from individuals with ATTRv-PN were examined by high-resolution electron microscopy and immunolabeling. The unit structure of the amyloid fibril is similar to the TTR monomer. This is consistent with the evidence that tetrameric TTR needs to dissociate to monomers to form amyloid.</p> <p>In the presence of <i>ex vivo</i> fibril extracts, TTR monomers are susceptible to nucleation and fibril formation. After fragmentation of fibrils, small fragments may serve as seeds that template fast polymerization.</p> <p>At 37°C, tetrameric TTR dissociates to a non-native monomer, which in turn depending on its conformational stability, may undergo partial unfolding that leads to aggregates formation and eventually amyloid fibril assembly, at TTR plasma concentrations. Both amyloidogenic and non-amyloidogenic TTR variants dissociate to non-native monomers. Amyloidogenic variants produce large amounts of partially unfolded monomeric species as a consequence of the marginal conformational stability of their non-native monomers, based on aging experiments. The aggregates formed by the amyloidogenic TTR variants show morphological and thioflavin-T fluorescence properties characteristic of amyloid fibrils.</p>	wt Val30Met Leu55Pro	TTR stock solutions in 10 mM phosphate, 100 mM KCl, 1 mM EDTA, pH 7.4, diluted in 50 mM sodium acetate or sodium phosphate, 100 mM KCl to acidic pH (5.0-3.9) to a final TTR concentration of 0.2 mg/mL (3.6 $\mu$ M).	Non-physiologic pH. Assumption that amyloid fibril formation <i>in vivo</i> occurs under acidic conditions in the lysosome. However, TTR amyloid deposits are extracellular.	[181,201]
	<p>Monomeric TTR intermediates undergo transient unfolding in some <math>\beta</math>-strands while retaining a stable <math>\beta</math>-sheet core, which could provide a starting point for amyloid fibril formation in TTRwt and its variants, at pH 4.5.</p> <p>At pH 2.0, TTR tetramers dissociate into denatured monomers. When adding 100 mM NaCl to denatured monomers, there is a change to an A-state or molten globule. In addition, these monomers present a denatured transformation of the compact deep globule type which has the ability to aggregate over time.</p> <p>Amyloid fibrils isolated from vitreous humor from individuals with ATTRv-PN were examined by high-resolution electron microscopy and immunolabeling. The unit structure of the amyloid fibril is similar to the TTR monomer. This is consistent with the evidence that tetrameric TTR needs to dissociate to monomers to form amyloid.</p> <p>In the presence of <i>ex vivo</i> fibril extracts, TTR monomers are susceptible to nucleation and fibril formation. After fragmentation of fibrils, small fragments may serve as seeds that template fast polymerization.</p>	wt Val30Met	TTR solutions at 0.005 mg/mL (0.09 $\mu$ M) prepared by a 100-fold dilution in water at pH 4.5, 37°C (pH adjusted with HCl).	Ionic strength and pH used in the experiment were not physiologic.	[202]
	<p>At pH 2.0, TTR tetramers dissociate into denatured monomers. When adding 100 mM NaCl to denatured monomers, there is a change to an A-state or molten globule. In addition, these monomers present a denatured transformation of the compact deep globule type which has the ability to aggregate over time.</p> <p>Amyloid fibrils isolated from vitreous humor from individuals with ATTRv-PN were examined by high-resolution electron microscopy and immunolabeling. The unit structure of the amyloid fibril is similar to the TTR monomer. This is consistent with the evidence that tetrameric TTR needs to dissociate to monomers to form amyloid.</p> <p>In the presence of <i>ex vivo</i> fibril extracts, TTR monomers are susceptible to nucleation and fibril formation. After fragmentation of fibrils, small fragments may serve as seeds that template fast polymerization.</p>	wt	TTR dialyzed against 10 mM HCl, pH 2.0, 4°C for 96 h. Aggregation of acid unfolded TTR at 3.5 $\mu$ M, 23°C induced by addition of NaCl to a final concentration of 100 mM.	Temperature and pH used in the experiment were not physiologic. No evidence in other TTR variants.	[203,204]
	<p>Amyloid fibrils isolated from vitreous humor from individuals with ATTRv-PN were examined by high-resolution electron microscopy and immunolabeling. The unit structure of the amyloid fibril is similar to the TTR monomer. This is consistent with the evidence that tetrameric TTR needs to dissociate to monomers to form amyloid.</p> <p>In the presence of <i>ex vivo</i> fibril extracts, TTR monomers are susceptible to nucleation and fibril formation. After fragmentation of fibrils, small fragments may serve as seeds that template fast polymerization.</p>	Val30Met	ATTRv30Met fibrils from biopsy samples of vitreous humor and kidney.	No evidence in other TTR variants.	[205]
	<p>In the presence of <i>ex vivo</i> fibril extracts, TTR monomers are susceptible to nucleation and fibril formation. After fragmentation of fibrils, small fragments may serve as seeds that template fast polymerization.</p>	Asp38Ala ( <i>ex vivo</i> fibril extracts)	Ex <i>in vivo</i> fibril extracts added to 0.5 mg/mL (9.1 $\mu$ M) TTRwt or to monomeric engineered TTR double mutant Phe87Met/Leu110Met, pH 4.3 and 7.4, respectively.	TTR concentrations and pH used in the experiments were not physiologic. Use of an engineered double TTR mutant (Phe87Met/Leu110Met).	[206]
	<p>At 37°C, tetrameric TTR dissociates to a non-native monomer, which in turn depending on its conformational stability, may undergo partial unfolding that leads to aggregates formation and eventually amyloid fibril assembly, at TTR plasma concentrations. Both amyloidogenic and non-amyloidogenic TTR variants dissociate to non-native monomers. Amyloidogenic variants produce large amounts of partially unfolded monomeric species as a consequence of the marginal conformational stability of their non-native monomers, based on aging experiments. The aggregates formed by the amyloidogenic TTR variants show morphological and thioflavin-T fluorescence properties characteristic of amyloid fibrils.</p>	wt Val30Met Leu55Pro Thr119Met	At physiological conditions: TTRwt and variants at CSF concentrations, in 20 mM sodium phosphate, 150 mM NaCl, pH 7.0, 37°C.	None.	[170, 207]

\*Amino acid numbering according to the 127-residue sequence of the mature protein, without the 20-residue signal peptide.

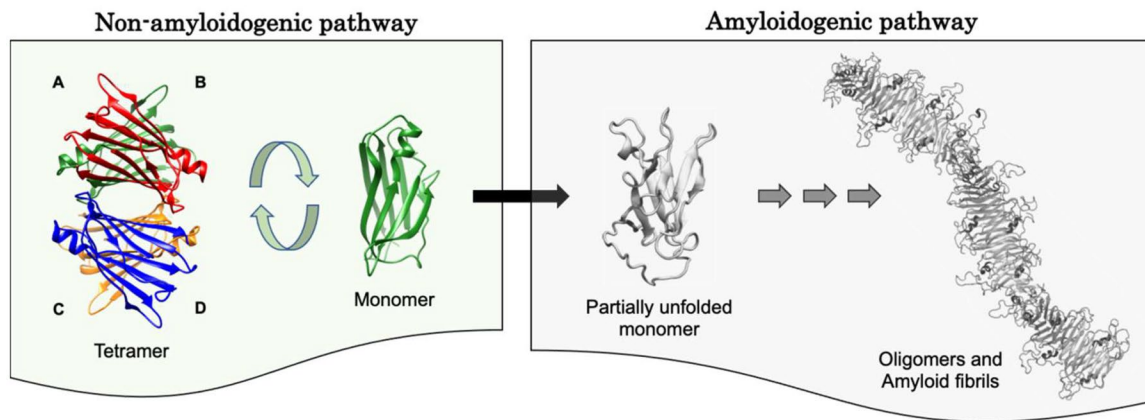


**Figure 5.** Transthyretin amyloid cascade. The tetrameric native form of TTR undergoes dissociation to a non-native monomer which upon partial unfolding and self-aggregation forms prefibrillar species, such as soluble oligomers and, eventually, mature amyloid fibrils.

### 3.3. Transthyretin structural fluctuations that promote fibrillogenesis

TTR amyloidogenesis is initiated by the dissociation of the native tetramer into monomers that undergo conformational fluctuations to partially unfolded intermediates, which self-assemble into soluble oligomers and amyloid fibrils [170]. Analysis of X-ray structures of tetrameric TTRwt and several of its natural variants revealed that both amyloidogenic and non-amyloidogenic mutations induce only minor changes in the overall three-dimensional structure of the protein [171,172]. Hence, single amino-acid substitutions must affect the conformational stability and folding/unfolding transitions of the protein rather than its overall structure [173]. The characterization of transient states populating the conformational ensemble between the natively folded functional TTR and aggregation-prone forms is of extreme relevance for understanding fibrillogenesis. The conformational changes identified as “amyloidogenic”, both by experimental and computational studies, point to structural perturbations occurring at different locations: the  $\alpha$ -helix and adjacent EF loop [174–177]; displacement of  $\beta$ -strands F, G, and H [178]; displacement of  $\beta$ -strands C and D from the  $\beta$ -sheet [179–184]; destabilization of the CBEF  $\beta$ -sheet [180]; destabilization of the CD loop [185] and FG loop [186]; proteolytic cleavage of Lys48–Thr49 peptide bond in the CD loop [187]; destabilization of the DAGH  $\beta$ -sheet [179,188–190]; and cooperative conformational transitions to  $\alpha$ -sheet of both TTR  $\beta$ -sheets [191,192]. Depending on the localization in the polypeptide chain and eventually the type of amino acid involved in the TTR amyloidogenic mutation, each one of these conformational changes may be related to local structural perturbations or partial unfolding, decreasing the conformational stability of the overall

molecule, and accelerating tetramer dissociation and subsequent monomer aggregation into oligomers and amyloid fibrils.

## 4. Transthyretin aggregation

### 4.1. Transthyretin aggregation models

Understanding the mechanism of TTR fibrillogenesis is critical for the rational design of therapeutic approaches aimed at retarding, preventing, and/or reverting amyloid formation and fibril deposition. Attempts to unravel the molecular mechanisms of TTR amyloidogenesis led to many experimental and theoretical studies over the years, and several models have emerged. The various models focused on the explanation of different aspects of the aggregation pathway, given the experimental conditions used, and contributed to the overall understanding of the process, complementing each other. Table 4 describes the main features underlying some of the models used to describe TTR aggregation in the past decades. Most models proposed the existence of a conformationally unstable intermediate that acquires conformational stability through aggregation, in the pathway to amyloid fibril formation [193,194]. Different starting oligomeric states have also been proposed over the years, from tetramers to dimers and monomers.

In the last two decades, a consensus has developed in the field that, in most instances, the molecular species that initiates the aggregation cascade is monomeric in nature (Table 4 and Figure 5). This implies tetramer dissociation to a monomeric intermediate as the first step of TTR fibril formation, followed by partial unfolding of the monomeric species and aggregation

Table 5. Transthyretin aggregation protocols.

pH	Temperature	Protocol description	Observations	TTR* variants	Binding of amyloid dyes	References
-	25°C	TTR dissolved in 50% TFE unbuffered solution.	Normally used in TTR fragments.	Tested in TTR(26-57).	N/S	[216]
-	25°C	TTR dissolved in 50% DMSO unbuffered solution.	Normally used in TTR fragments.	Tested in TTR(26-57).	N/S	[216]
2.0	25°C	TTR dissolved in 10 mM HCl, 5 mM SDS.	Normally used in TTR fragments.	Tested in TTR(26-57).	ThT positive	[216]
2.0	4°C and then change to 25°C	TTR prepared by dialysis against 10 mM HCl for 96 h, pH 2.0 at 4°C. TTR aggregation induced by addition of NaCl to a final concentration of 100 mM.	The protocol separates the unfolding and aggregation steps.	Used in TTRwt, but also recommended for TTR amyloidogetic variants.	DCVJ and ThT positive	[203,217]
2.0	37°C and then change to 25°C	TTR dissolved in 10% acetonitrile, with pH adjusted to pH 2.0, with HCl. Samples are kept at 37°C for 2 days and then incubated at 25°C, for 2 weeks.	Normally used in TTR fragments.	Tested in TTR(10-20), TTR(105-115) and TTR(105-115) <sup>Leu111Met</sup> .	N/S	[218,219]
2.0 (up to 3.7)	37°C	TTR solution in 50 mM maleic acid and 100 mM KCl, first diluted in pH 2.0, and after 30 min the pH is raised to 3.7, by the addition of a predetermined volume of 2 M KOH.	-	Recommended for TTR amyloidogetic variants, but also TTRwt.	CR positive	[197]
2.3	25°C	TTR dissolved in 10% acetic acid.	Normally used in TTR fragments.	Tested in TTR(10-20), TTR(105-115), TTR(105-115) <sup>Leu111Met</sup> , TTR(115-124) and TTR(115-127).	CR positive	[218,220,221]
2.5 (up to 3.6)	0°C and then change to 37°C	pH of the TTR solution lowered to pH 2.5, with HCl at 0°C, incubated for 20 min. The pH is rapidly increased by adding a fixed amount of NaOH, to bring the solution to pH 3.6.	-	Recommended for TTR amyloidogetic variants, but also TTRwt.	CR positive	[222]
3.0	4°C	TTR dissolved in 50 mM acetic acid and 100 mM NaCl.	-	Recommended for TTR amyloidogetic variants, but also TTRwt.	ThT positive	[223]
3.6	25°C or 37°C	TTR dissolved in 50 mM glycine buffer or in 50 mM sodium acetate buffer.	-	Recommended for TTR amyloidogetic variants, but also TTRwt.	ThT positive	[224,225]
3.9–5.0	37°C	TTR solution (10 mM sodium phosphate, pH 7.2 or 7.4, 100 mM KCl, and 1 mM EDTA) two-fold diluted with 50 mM sodium acetate buffer, 100 mM KCl, 1 mM EDTA to the desired pH. The mixture is incubated for 72 h and the TTR final concentration is 3.6 µM.	The pH extent and the maximal pH of amyloid fibril formation depends on the TTR variant used in the assay. This protocol was also adapted to a HTS format using 96-well microplates.	Recommended for TTR amyloidogetic variants, but also TTRwt.	CR positive	[181,211,226]
4.3	37°C	Ex vivo fibril extracts added to 0.5 mg/mL recombinant TTRwt, in 10 mM sodium acetate, 100 mM KCl, 1 mM EDTA.	Used of ex vivo purified seeds from ATTRv patient.	Ex vivo fibril extracts of TTRAsp38Ala used as seeds for aggregation of recombinant TTRwt.	ThT positive	[227]
5.0	25°C	TTR solution in 100 mM MES, 100 mM KCl, pH 5.0, mixed with heparin at a protein:polymer ratio of 1:0.1, 1:0.2, or 1:0.3.	Immediate TTR amyloid fibril formation. Heparin is known to enhance the aggregation propensity.	Tested in TTR(26-57).	ThT positive	[216]
5.0–5.6	37°C	TTR in 50 mM MES, 100 mM KCl at acidic pH, compressed at 3000 bar (1 bar = 100 kPa) for 30 min. After this period, pressure is released.	After pressure release, TTR undergoes aggregation.	Recommended for TTR amyloidogetic variants, but also TTRwt.	CR positive	[228]
7.0	4°C followed by heating to 37°C	TTR dialyzed against water and concentrated to 5 mg/mL. The preparation is centrifuged (15,000 g, 30 min, 4°C), the pellet is resuspended in PBS or 0.9% NaCl at 2 mg/mL, and the sample is then incubated at 37°C.	The centrifugation step separates dimeric and the aggregates species.	Recommended for highly TTR amyloidogetic variants.	ThT positive	[229]
7.0	25°C	TTR dissolved in 10% acetic acid and neutralized to pH 7.0, with NH <sub>3</sub> .	Normally used in TTR fragments.	Tested in TTR(105-115).	N/S	[218]
7.0	25°C	TTR dissolved in 1% acetic acid.	Normally used in TTR fragments.	Tested in TTR(28-33) <sup>Val30Met</sup> .	CR and ThT positive	[230]

(Continued)

Table 5. Continued.

pH	Temperature	Protocol description	Observations	TTR* variants	Binding of amyloid dyes	References
7.0	55 °C – 65 °C	TTR in 20 mM potassium phosphate buffer, incubated for 72 to 96h.	The maximal temperature of amyloid fibril formation might depend on the TTR variant or TTR-related protein used in the assay.	Tested in TTR-related proteins, but also in TTRwt.	CR positive	[182,231]
7.4	37 °C	Ex vivo fibril extracts were added to 0.5 mg/mL recombinant TTRwt, in 10 mM sodium phosphate, 100 mM KCl, 1 mM EDTA.	Used of ex vivo purified seeds from ATTRv patient. Initial lag phase followed by immediate TTR fibril formation.	Ex vivo fibril extracts of TTRAsp38Ala used as seeds for aggregation of monomeric engineered TTR double Phe87/Met/Leu110Met mutant.	ThT positive	[227]
7.4	37 °C	TTR aggregation was carried out in proper glass vials stirred at 1,500 rpm in PBS for 72h, in the presence of trypsin at an enzyme:substrate ratio of 1:200.	The use of protease trypsin cleaves TTR and releases the TTR(49-127) fragment that is prone to aggregate. Fibrillogenesis requires the action of biomechanical forces provided by the shear stress of physiological fluid flow. This protocol can be used in a HTS format using 96-well microplates.	Recommended for TTR amyloidogenic variants, but also TTRwt.	CR and ThT positive	[232]
7.4	37 °C	TTR solution in 20 mM Tris-HCl, 150 mM NaCl, 5 mM CaCl <sub>2</sub> , incubated with plasmin at an enzyme:substrate ratio of 1:50 and stirred at 900 rpm.	The use of protease plasmin cleaves TTR and releases the TTR(49-127) fragment that is prone to aggregate. This protocol can be used in a HTS format using 96-well microplates.	Recommended for TTR amyloidogenic variants, but also TTRwt.	CR and ThT positive	[233]
7.4	37 °C	TTR dissolved in PBS.	Normally used in TTR fragments.	Tested in TTR(12-17), TTR(25-30), TTR(26-32), TTR(28-33), TTR(47-52), TTR(65-70), TTR(68-73), TTR(80-85), TTR(91-96), TTR(105-110), TTR(106-112) and TTR(119-124).	N/S	[234]
7.4	37 °C	TTR at 5–15 mg/mL in PBS were incubated under constant agitation at 250 rpm.	Fibrillogenesis requires the action of biomechanical forces provided by the shear stress of the physiological fluid flow.	Recommended for TTR amyloidogenic variants, but also TTRwt.	N/S	[235]
7.4	37 °C	TTR incubated in PBS for 72 h, followed by 5 min of vigorous stirring.	In the case of TTRwt, the incubation is 96 h, followed by 25 min of vigorous stirring.	Recommended for TTR amyloidogenic variants, but also TTRwt.	N/S	[236]

N/S: not sufficient information. \* Amino acid numbering according to the 127-residue sequence of the mature protein, without the 20-residue signal peptide.

into amyloid. Since tetramer dissociation is the first step toward TTR amyloid formation and the rate-limiting step for fibrillogenesis [208], it is paramount to characterize the dissociation pathway. The quaternary structure of TTR contains two distinct dimer-dimer interfaces – AB/CD and AC/BD, interfaces between transversal and longitudinal dimers, respectively (Figures 1 and 5). Several pathways may be envisaged for the dissociation of a homotetrameric protein. However, the dissociation mechanism reported for TTR consists of an initial AB/CD dimer-dimer scission followed by a rapid dissociation of dimers into monomers [208]. This dissociation mechanism also rationalizes and points toward the relevance of stabilizing the tetrameric conformation by small molecule binding to the natural thyroxine binding sites which are located in the AB/CD dimer-dimer interface, according to one of the therapeutic approaches currently available to ATTR patients [209]. Conversely, the refolding mechanism from unfolded monomers to native tetramers comprises a single intermediate with monomeric characteristics [210].

#### 4.2. Transthyretin aggregation protocols

Several studies on the aggregation pathway of TTR have demonstrated that amyloid fibril formation is preceded by the dissociation of the native tetramer into non-native monomers that self-assemble into non-fibrillar cytotoxic oligomers, which are prone to form protofibrils and elongate into mature amyloid fibrils. Table 5 lists the various TTR aggregation protocols reported in the literature. These are not only useful to study aggregation mechanisms but also to screen for potential aggregation inhibitors [211,212] and modulators [213,214]. The experimental conditions of these aggregation protocols vary widely with some making use of proteolytic cleavage, organic solvents, and temperature, while others submit the protein to sample aging, high pressure, low pH, changes in ionic strength, or use a combination of these destabilizing effects. TTR aggregation species formed *in vitro* have many morphological and tinctorial properties common to amyloid material found *in vivo*, and may therefore be used to study TTR fibrillation leading to ATTR amyloidosis [215]. Depending on the goals of a particular study, different experimental conditions and protocols may be used, but it must be kept in mind that the kinetics of the processes and the structural and oligomeric features of the intermediate and final species vary. In particular, it must be stressed that the coexistence of different relative amounts of well-structured amyloid aggregates and amorphous aggregates varies

significantly from condition to condition and protocol to protocol.

## 5. Conclusions

Transthyretin (TTR) is a transport protein for thyroid hormones (THs) and retinol in association with the retinol-binding protein (RBP). Nevertheless, TTR may exhibit additional biological functions albeit less known. More than 200 TTR natural variants have already been identified and most of them are pathogenic (~93%). Hereditary transthyretin amyloidosis polyneuropathy (ATTRv-PN) and hereditary transthyretin amyloidosis cardiomyopathy (ATTRv-CM) are the most common clinical manifestations of hereditary ATTR. Additionally, wild-type TTR also forms amyloid leading to ATTRwt, a mainly age-related progressive cardiomyopathy with poor prognosis and characterized by heart failure. Among human proteins, TTR has a high rate of mutations leading to amyloid fibril formation. An average of 1.7 point mutations (216 mutations in total) have been identified per residue of the TTR polypeptide chain subunit (with 127 residues). TTR amyloid fibrils are highly stable  $\beta$ -structured protein aggregates. Different pathogenic TTR mutations can produce different phenotypes, with different clinical manifestations and targeted organs, either leading to polyneuropathy, cardiomyopathy, vitreous opacities, carpal tunnel syndrome, CNS dysfunction, or leptomeningeal involvement. Genotype–phenotype correlations are not only due to specific triggering mutations but distinct pathological phenotypes within different populations are observed for the same TTR mutated genotype. Most mutations result in single amino acid substitutions. “Hot spot” mutation regions are largely assigned to  $\beta$ -strands B, C, and D. The most aggressive amyloidogenic mutations are mainly localized in the 44-59 segment of the protein sequence, whereas non-amyloidogenic mutations are mostly located in the 97-125 segment. Aspartic acid is the most mutated residue, followed by arginine, isoleucine, phenylalanine, and alanine. Tryptophan, asparagine, proline, and lysine residues show high conservation propensities along the protein sequence.

TTR fibrillogenesis occurs upon tetramer dissociation and partial unfolding to non-native monomers that undergo self-assembly into cytotoxic soluble oligomers and then into mature amyloid fibril deposits. Monomeric TTR species have been identified as crucial intermediates in amyloid fibril formation, either by wild-type TTR (TTRwt) or by other amyloidogenic TTR variants (TTRv). TTR fibrillogenesis can be rapidly and efficiently reproduced *in vitro* through various

experimental protocols taking advantage of different experimental conditions using proteolytic cleavage, organic solvents, high temperature, sample aging, high pressure, low pH, changes in ionic strength, or a combination of these protein destabilizing effects. These different experimental conditions, however, produce different oligomeric species, and in particular, different proportions of amyloid and amorphous aggregates, which must be considered when studying fundamental processes in protein aggregation and amyloidogenesis and when screening for amyloid inhibitors and modulators in drug discovery and development.

### Disclosure statement

The authors report there are no competing interests to declare.

### Funding

This work was supported by COMPETE and CENTRO-202010.13039/501100011929 and by Fundação para a Ciência e a Tecnologia (FCT) through grants UIDB/00313/2020 and UIDP/00313/2020 (to Coimbra Chemistry Center, University of Coimbra) and doctoral fellowship SFRH/BD/137991/2018 (to Z.L.A.).

### References

- [1] Almeida ZL, Brito RMM. Structure and aggregation mechanisms in amyloids. *Molecules*. 2020;25(5):1195. doi:10.3390/molecules25051195.
- [2] Seibert FB, Nelson JW. Electrophoretic study of the blood protein response in tuberculosis. *J Biol Chem*. 1942;143(1):29–38. doi:10.1016/s0021-9258(18)72655-0.
- [3] Kabat EA, Moore DH, Landow H. An electrophoretic study of the protein components in cerebrospinal fluid and their relationship to the serum proteins 1. *J Clin Invest*. 1942;21(5):571–577. doi:10.1172/jci101335.
- [4] Ingbar SH. Pre-albumin: a thyroxine-binding protein of human plasma. *Endocrinology*. 1958;63(2):256–259. doi:10.1210/endo-63-2-256.
- [5] Raz A, Goodman DS. The interaction of thyroxine with human plasma prealbumin and with the prealbumin-retinol-binding protein complex. *J Biol Chem*. 1969;244(12):3230–3237. doi:10.1016/s0021-9258(18)93118-2.
- [6] Nomenclature Committee of the International Union of Biochemistry (NC-IUB). Enzyme nomenclature. Recommendations 1978. Supplement 2: corrections and additions. *Eur J Biochem*. 1981;116(3):423–435.
- [7] Smith FR, Goodman DS. The effects of diseases of the liver, thyroid, and kidneys on the transport of vitamin a in human plasma. *J Clin Invest*. 1971;50(11):2426–2436. doi:10.1172/JCI106741.
- [8] Ramström M, Bergquist J. Proteomics of human cerebrospinal fluid. In *Proteomics of human body fluids: principles, methods, and applications*. Totowa (NJ): humana Press Inc.; 2007:269–284. doi:10.1007/978-1-59745-432-2\_12.
- [9] Aleshire SL, Bradley CA, Richardson LD, et al. Localization of human prealbumin in choroid plexus epithelium. *J Histochem Cytochem*. 1983;31(5):608–612. doi:10.1177/31.5.6341455.
- [10] Dickson PW, Schreiber G. High levels of messenger RNA for transthyretin (prealbumin) in human choroid plexus. *Neurosci Lett*. 1986;66(3):311–315. doi:10.1016/0304-3940(86)90037-6.
- [11] Vatassery GT, Quach HT, Smith WE, et al. A sensitive assay of transthyretin (prealbumin) in human cerebrospinal fluid in nanogram amounts by ELISA. *Clin Chim Acta*. 1991;197(1):19–25. doi:10.1016/0009-8981(91)90344-C.
- [12] Martone RL, Herbert J, Dwork A, et al. Transthyretin is synthesized in the mammalian eye. *Biochem Biophys Res Commun*. 1988;151(2):905–912. doi:10.1016/S0006-291X(88)80367-X.
- [13] Getz RK, Kennedy BG, Mangini NJ. Transthyretin localization in cultured and native human retinal pigment epithelium. *Exp Eye Res*. 1999;68(5):629–636. doi:10.1006/exer.1998.0646.
- [14] Dwork AJ, Cavallaro T, Martone RL, et al. Distribution of transthyretin in the rat eye. *Invest Ophthalmol Vis Sci*. 1990;31(3):489–496.
- [15] Grus FH, Joachim SC, Sandmann S, et al. Transthyretin and complex protein pattern in aqueous humor of patients with primary open-angle glaucoma. *Mol Vis*. 2008;14:1437–1445.
- [16] Van Aken E, De Letter EA, Veckeneer M, et al. Transthyretin levels in the vitreous correlate with change in visual acuity after vitrectomy. *Br J Ophthalmol*. 2009;93(11):1539–1545. doi:10.1136/bjo.2009.158048.
- [17] Murakami T, Ohsawa Y, Zhenghua L, et al. The transthyretin gene is expressed in Schwann cells of peripheral nerves. *Brain Res*. 2010;1348:222–225. doi:10.1016/j.brainres.2010.06.017.
- [18] Li X, Masliah E, Reixach N, et al. Neuronal production of transthyretin in human and murine Alzheimer's disease: is it protective? *J Neurosci*. 2011;31(35):12483–12490. doi:10.1523/jneurosci.2417-11.2011.
- [19] Pettersen EF, Goddard TD, Huang CC, et al. UCSF Chimera - a visualization system for exploratory research and analysis. *J Comput Chem*. 2004;25(13):1605–1612. doi:10.1002/jcc.20084.
- [20] Soprano DR, Herbert J, Soprano KJ, et al. Demonstration of transthyretin mRNA in the brain and other extrahepatic tissues in the rat. *J Biol Chem*. 1985;260(21):11793–11798. doi:10.1016/s0021-9258(17)39100-7.
- [21] Soprano DR, Soprano KJ, Goodman DS. Retinol-binding protein and transthyretin mRNA levels in visceral yolk sac and liver during fetal development in the rat. *Proc Natl Acad Sci U S A*. 1986;83(19):7330–7334. doi:10.1073/pnas.83.19.7330.
- [22] McKinnon B, Li H, Richard K, et al. Synthesis of thyroid hormone binding proteins transthyretin and albumin by human trophoblast. *J Clin Endocrinol Metab*. 2005;90(12):6714–6720. doi:10.1210/jc.2005-0696.
- [23] Walker AK, Gong Z, Park WM, et al. Expression of serum retinol binding protein and transthyretin within

- mouse gastric ghrelin cells. Luque RM, ed. *PLoS One*. 2013;8(6):e64882. doi:10.1371/journal.pone.0064882.
- [24] Martone RL, Mizuno R, Herbert J. The mammalian pineal gland is a synthetic site for TTR and RBP. *J Rheumatol*. 1993;20:175.
- [25] Blay P, Nilsson C, Hansson S, et al. An in vivo study of the effect of 5-HT and sympathetic nerves on transferrin and transthyretin mRNA expression in rat choroid plexus and meninges. *Brain Res*. 1994;662(1-2):148–154. doi:10.1016/0006-8993(94)90807-9.
- [26] Jacobsson B, Collins VP, Grimelius L, et al. Transthyretin immunoreactivity in human and porcine liver, choroid plexus, and pancreatic islets. *J Histochem Cytochem*. 1989;37(1):31–37. doi:10.1177/37.1.2642294.
- [27] Jacobsson B. In situ localization of transthyretin-mRNA in the adult human liver, choroid plexus and pancreatic islets and in endocrine tumours of the pancreas and gut. *Histochemistry*. 1989;91(4):299–304. doi:10.1007/BF00493004.
- [28] Ingenbleek Y, De Visscher M. Hormonal and nutritional status: critical conditions for endemic goiter epidemiology? *Metabolism*. 1979;28(1):9–19. doi:10.1016/0026-0495(79)90162-8.
- [29] Socolow EL, Woeber KA, Purdy RH, et al. Preparation of I-131-labeled human serum prealbumin and its metabolism in normal and sick patients. *J Clin Invest*. 1965;44(10):1600–1609. doi:10.1172/JCI105266.
- [30] Ando Y, Tanaka Y, Nakazato M, et al. Change in variant transthyretin levels in patients with familial amyloidotic polyneuropathy type I following liver transplantation. *Biochem Biophys Res Commun*. 1995;211(2):354–358. doi:10.1006/bbrc.1995.1820.
- [31] Makover A, Moriwaki H, Ramakrishnan R, et al. Tissue sites of degradation and turnover in the rat. *J Biol Chem*. 1988;263(18):8598–8603. doi:10.1016/s0021-9258(18)68346-2.
- [32] Ritchie RF, Palomaki GE, Neveux LM, et al. Reference distributions for the negative acute-phase proteins, albumin, transferrin, and transthyretin: a comparison of a large cohort to the world's literature. *J Clin Lab Anal*. 1999;13(6):280–286. doi:10.1002/(SICI)1098-2825(1999)13:6<280::AID-JCLA5>3.0.CO;2-U.
- [33] Johnson AM, Merlini G, Sheldon J, et al. Clinical indications for plasma protein assays: transthyretin (prealbumin) in inflammation and malnutrition. *Clin Chem and Lab Med*. 2007;45(3):419–426. doi:10.1515/CCLM.2007.051.
- [34] Féraud G, Gaudias J, Bourguignat A, et al. C-reactive protein to transthyretin ratio for the early diagnosis and follow-up of postoperative infection. *Clin Chem Lab Med*. 2002;40(12):1334–1338. doi:10.1515/CCLM.2002.230.
- [35] Ingenbleek Y, Young VR. Significance of transthyretin in protein metabolism. *Clin Chem Lab Med*. 2002;40(12):1281–1291. doi:10.1515/CCLM.2002.222.
- [36] Gloeckner SF, Meyne F, Wagner F, et al. Quantitative analysis of transthyretin, tau and amyloid- $\beta$  in patients with dementia. *J Alzheimer's Dis*. 2008;14(1):17–25. doi:10.3233/JAD-2008-14102.
- [37] Liu M, Chen Y, Chen D. Association between transthyretin concentrations and gestational diabetes mellitus in Chinese women. *Arch Gynecol Obstet*. 2020;302(2):329–335. doi:10.1007/s00404-020-05599-y.
- [38] Heywood W, Mills K, Wang D, et al. Identification of new biomarkers for Down's syndrome in maternal plasma. *J Proteomics*. 2012;75(9):2621–2628. doi:10.1016/j.jprot.2012.03.007.
- [39] Kharb, Rupsi, Sharma, Ankita, Chaddar, Monu Kumar, et al. Plasma proteome profiling of coronary artery disease patients: downregulation of transthyretin—an important event. *Mediators Inflamm*. 2020;2020:3429541. doi:10.1155/2020/3429541.
- [40] Oppenheimer JH. Role of plasma proteins in the binding, distribution and metabolism of the thyroid hormones. *N Engl J Med*. 1968;278(21):1153–1162. doi:10.1056/nejm196805232782107.
- [41] Mendel CM. The free hormone hypothesis: a physiologically based mathematical model. *Endocr Rev*. 1989;10(3):232–274. doi:10.1210/edrv-10-3-232.
- [42] Janssen ST, Janssen OE. Directional thyroid hormone distribution via the blood stream to target sites. *Mol Cell Endocrinol*. 2017;458:16–21. doi:10.1016/j.mce.2017.02.037.
- [43] Chang L, Munro SLA, Richardson SJ, et al. Evolution of thyroid hormone binding by transthyretins in birds and mammals. *Eur J Biochem*. 1999;259(1-2):534–542. doi:10.1046/j.1432-1327.1999.00076.x.
- [44] Itrace G, Edelhoch H. Thyroxine-induced conformational changes in prealbumin. *Biochemistry*. 1978;17(26):5729–5733. doi:10.1021/bi00619a020.
- [45] Benvenga S, Robbins J. Enhancement of thyroxine entry into low density lipoprotein (LDL) receptor-Competent fibroblasts by LDL: an additional mode of entry of thyroxine into cells. *Endocrinology*. 1990;126(2):933–941. doi:10.1210/endo-126-2-933.
- [46] Benvenga S, Cahnmann H, Gregg R, et al. Binding of thyroxine to human plasma low density lipoprotein through specific interaction with apolipoprotein B (apoB-100). *Biochimie*. 1989;71(2):263–268. doi:10.1016/0300-9084(89)90063-1.
- [47] Richardson SJ, Wijayagunaratne RC, D'Souza DG, et al. Transport of thyroid hormones via the choroid plexus into the brain: the roles of transthyretin and thyroid hormone transmembrane transporters. *Front Neurosci*. 2015;9(MAR):66. doi:10.3389/fnins.2015.00066.
- [48] Ronne H, Ocklind C, Wiman K, et al. Ligand-dependent regulation of intracellular protein transport: effect of vitamin a on the secretion of the retinol-binding protein. *J Cell Biol*. 1983;96(3):907–910. doi:10.1083/jcb.96.3.907.
- [49] Monaco HL, Rizzi M, Coda A. Structure of a complex of two plasma proteins: transthyretin and retinol-binding protein. *Science*. 1995;268(5213):1039–1041. doi:10.1126/science.7754382.
- [50] Naylor HM, Newcomer ME. The structure of human retinol-binding protein (RBP) with its carrier protein transthyretin reveals an interaction with the carboxy terminus of RBP. *Biochemistry*. 1999;38(9):2647–2653. doi:10.1021/bi982291i.
- [51] Fex G, Albertsson PA, Hansson B. Interaction between prealbumin and retinol-binding protein studied by affinity chromatography, gel filtration and two-Phase partition. *Eur J Biochem*. 1979;99(2):353–360. doi:10.1111/j.1432-1033.1979.tb13263.x.
- [52] Goodman DS. Vitamin a transport and retinol-binding protein metabolism. *Vitam Horm*. 1975;32(C):167–180. doi:10.1016/S0083-6729(08)60011-4.

- [53] Kopelman M, Cogan U, Mokady S, et al. The interaction between retinol-binding proteins and prealbumins studied by fluorescence polarization. *Biochim Biophys Acta*. 1976;439(2):449–460. doi:10.1016/0005-2795(76)90082-9.
- [54] Rostom AA, Sunde M, Richardson SJ, et al. Dissection of multi-protein complexes using mass spectrometry: subunit interactions in transthyretin and retinol-binding protein complexes. *Proteins*. 1998;33(S2):3–11. doi:10.1002/(SICI)1097-0134(1998)33:2+ <3::AID-PROT2 >3.0.CO;2-H.
- [55] Shoji S, Nakagawa S. Serum prealbumin and retinol-binding protein concentrations in Japanese-Type familial amyloid polyneuropathy. *Eur Neurol*. 1988; 28(4):191–193. doi:10.1159/000116264.
- [56] Filteau SM, Willumsen JF, Sullivan K, et al. Use of the retinol-binding protein: transthyretin ratio for assessment of vitamin a status during the acute-phase response. *Br J Nutr*. 2000;83(5):513–520. doi:10.1017/S0007114500000659.
- [57] Prashantha DK, Taly AB, Sinha S, et al. Familial amyloidotic polyneuropathy with muscle, vitreous, leptomeningeal, and cardiac involvement: phenotypic, pathological, and MRI description. *Ann Indian Acad Neurol*. 2010;13(2):142–144. doi:10.4103/0972-2327.64642.
- [58] Brett M, Persey MR, Reilly MM, et al. Transthyretin Leu12Pro is associated with systemic, neuropathic and leptomeningeal amyloidosis. *Brain*. 1999;122 (Pt 2)(2):183–190. doi:10.1093/brain/122.2.183.
- [59] McColgan P, Viegas S, Gandhi S, et al. Oculoleptomeningeal amyloidosis associated with transthyretin Leu12Pro in an African patient. *J Neurol*. 2015;262(1):228–234. doi:10.1007/s00415-014-7594-2.
- [60] Dispenzieri A, Coelho T, Conceição I, et al. A consolidated overview of 14 years of global data from the transthyretin amyloidosis outcomes survey. *J Card Fail*. 2022;28(5):S111. doi:10.1016/j.cardfail.2022.03.284.
- [61] Dzungu JN, Anderson LJ, Whelan CJ, et al. Cardiac transthyretin amyloidosis. *Heart*. 2012;98(21):1546–1554. doi:10.1136/heartjnl-2012-301924.
- [62] Ruberg FL, Grogan M, Hanna M, et al. Transthyretin amyloid cardiomyopathy: JACC state-of-the-Art review. *J Am Coll Cardiol*. 2019;73(22):2872–2891. doi:10.1016/j.jacc.2019.04.003.
- [63] Maurer MS, Elliott P, Comenzo R, et al. Addressing common questions encountered in the diagnosis and management of cardiac amyloidosis. *Circulation*. 2017;135(14):1357–1377. doi:10.1161/circulationaha.116.024438.
- [64] Ueda M, Horibata Y, Shono M, et al. Clinicopathological features of senile systemic amyloidosis: an ante-and post-mortem study. *Mod Pathol*. 2011;24(12):1533–1544. doi:10.1038/modpathol.2011.117.
- [65] González-López E, Gallego-Delgado M, Guzzo-Merello G, et al. Wild-type transthyretin amyloidosis as a cause of heart failure with preserved ejection fraction. *Eur Heart J*. 2015;36(38):2585–2594. doi:10.1093/eurheartj/ehv338.
- [66] Ternacle J, Krapf L, Mohty D, et al. Aortic stenosis and cardiac amyloidosis. *J Am Coll Cardiol*. 2019;74(21):2638–2651. doi:10.1016/j.jacc.2019.09.056.
- [67] Hafeez AS, Bavry AA. Diagnosis of transthyretin amyloid cardiomyopathy. *Cardiol Ther*. 2020;9(1):85–95. doi:10.1007/s40119-020-00169-4.
- [68] Grogan M, Scott CG, Kyle RA, et al. Natural history of wild-type transthyretin cardiac amyloidosis and risk stratification using a novel staging system. *J Am Coll Cardiol*. 2016;68(10):1014–1020. doi:10.1016/j.jacc.2016.06.033.
- [69] Ghosh S, Khanra D, Krishna V, et al. Wild type transthyretin cardiac amyloidosis in a young individual: a case report. *Medicine (Baltimore)*. 2021;100(17):e25462. doi:10.1097/MD.00000000000025462.
- [70] Connors LH, Sam F, Skinner M, et al. Heart failure resulting from age-related cardiac amyloid disease associated with wild-type transthyretin: a prospective, observational cohort study. *Circulation*. 2016;133(3):282–290. doi:10.1161/circulationaha.115.018852.
- [71] Schmidt HH, Waddington-Cruz M, Botteman MF, et al. Estimating the global prevalence of transthyretin familial amyloid polyneuropathy. *Muscle Nerve*. 2018; 57(5):829–837. doi:10.1002/mus.26034.
- [72] Zhen DB, Swiecicki PL, Zeldenrust SR, et al. Frequencies and geographic distributions of genetic mutations in transthyretin- and non-transthyretin-related familial amyloidosis. *Clin Genet*. 2015;88(4):396–400. doi:10.1111/cge.12500.
- [73] Soares ML, Coelho T, Sousa A, et al. Haplotypes and DNA sequence variation within and surrounding the transthyretin gene: genotype-phenotype correlations in familial amyloid polyneuropathy (V30M) in Portugal and Sweden. *Eur J Hum Genet*. 2004;12(3):225–237. doi:10.1038/sj.ejhg.5201095.
- [74] Jacobson DR, Alexander AA, Tagoe C, et al. Prevalence of the amyloidogenic transthyretin (TTR) V122I allele in 14 333 African-Americans. *Amyloid*. 2015;22(3):171–174. doi:10.3109/13506129.2015.1051219.
- [75] Jacobson DR, Alexander AA, Tagoe C, et al. The prevalence and distribution of the amyloidogenic transthyretin (TTR) V122I allele in Africa. *Mol Genet Genomic Med*. 2016;4(5):548–556. doi:10.1002/mgg3.231.
- [76] Dzungu JN, Papadopoulou SA, Wykes K, et al. Afro-Caribbean heart failure in the United Kingdom. *Circ: heart Failure*. 2016;9(9):e003352. doi:10.1161/CIRCHEARTFAILURE.116.003352.
- [77] Arruda-Olson AM, Zeldenrust SR, Dispenzieri A, et al. Genotype, echocardiography, and survival in familial transthyretin amyloidosis. *Amyloid*. 2013;20(4):263–268. doi:10.3109/13506129.2013.845745.
- [78] Dharmarajan K, Maurer MS. Transthyretin cardiac amyloidosis in older North Americans. *J Am Geriatr Soc*. 2012;60(4):765–774. doi:10.1111/j.1532-5415.2011.03868.x.
- [79] Gillmore JD, Maurer MS, Falk RH, et al. Nonbiopsy diagnosis of cardiac transthyretin amyloidosis. *Circulation*. 2016;133(24):2404–2412. doi:10.1161/circulationaha.116.021612.
- [80] Fan K, Zhu H, Xu H, et al. The identification of a transthyretin variant p.D38G in a Chinese family with early-onset leptomeningeal amyloidosis. *J Neurol*. 2019;266(1):232–241. doi:10.1007/s00415-018-9125-z.
- [81] Mitsuhashi S, Yazaki M, Tokuda T, et al. Biochemical characteristics of variant transthyretins causing hereditary leptomeningeal amyloidosis. *Amyloid*. 2005; 12(4):216–225. doi:10.1080/13506120500352404.
- [82] Martins AC, Rosa AM, Costa E, et al. Ocular manifestations and therapeutic options in patients with familial amyloid polyneuropathy: a systematic review. *Biomed Res Int*. 2015;2015:282405–282409. doi:10.1155/2015/282405.

- [83] Dammacco R, Merlini G, Lisch W, et al. Amyloidosis and ocular involvement: an overview. *Semin Ophthalmol*. 2020;35(1):7–26. doi:10.1080/08820538.2019.1687738.
- [84] Beirão JM, Malheiro J, Lemos C, et al. Impact of liver transplantation on the natural history of oculopathy in Portuguese patients with transthyretin (V30M) amyloidosis. *Amyloid*. 2015;22(1):31–35. doi:10.3109/13506129.2014.989318.
- [85] Hara R, Kawaji T, Ando E, et al. Impact of liver transplantation on transthyretin-related ocular amyloidosis in Japanese patients. *Arch Ophthalmol*. 2010;128(2):206–210. doi:10.1001/archophthalmol.2009.390.
- [86] Reddi HV, Jenkins S, Theis J, et al. Homozygosity for the V122I mutation in transthyretin is associated with earlier onset of cardiac amyloidosis in the African American population in the seventh decade of life. *J Mol Diagn*. 2014;16(1):68–74. doi:10.1016/j.jmoldx.2013.08.001.
- [87] Maia LF, Magalhães R, Freitas J, et al. CNS involvement in V30M transthyretin amyloidosis: clinical, neuropathological and biochemical findings. *J Neurol Neurosurg Psychiatry*. 2015;86(2):159–167. doi:10.1136/JNNP-2014-308107.
- [88] Benson MD, Kincaid JC. The molecular biology and clinical features of amyloid neuropathy. *Muscle Nerve*. 2007;36(4):411–423. doi:10.1002/mus.20821.
- [89] Wang Y, Wang Q, Huang H, et al. A crowdsourcing open platform for literature curation in UniProt. *PLoS Biol*. 2021;19(12):e3001464. doi:10.1371/journal.pbio.3001464.
- [90] Andrade C. A peculiar form of peripheral neuropathy: familiar atypical generalized amyloidosis with special involvement of the peripheral nerves. *Brain*. 1952;75(3):408–427. doi:10.1093/brain/75.3.408.
- [91] Araki S, Mawatari S, Ohta M, et al. Polyneuritic amyloidosis in a Japanese family. *Arch Neurol*. 1968;18(6):593–602. doi:10.1001/archneur.1968.00470360015001.
- [92] Andersson R. Familial amyloidosis with polyneuropathy. A clinical study based on patients living in northern Sweden [dissertation]. Umeå (SE): Umeå Universitet; 1976.
- [93] Jinnō Y, Matsumoto T, Kamel T, et al. Localization of the human prealbumin gene to 18p11.1-q12.3 by gene dose effect study of Southern blot hybridization. *Jinrui Idengaku Zasshi*. 1986;31(3):243–248. doi:10.1007/BF01870754.
- [94] Hiroyuki S, Naoko Y, Yasuyuki T, et al. Structure of the chromosomal gene for human serum prealbumin. *Gene*. 1985;37(1-3):191–197. doi:10.1016/0378-1119(85)90272-0.
- [95] Rowczenio DM, Noor I, Gillmore JD, et al. Online registry for mutations in hereditary amyloidosis including nomenclature recommendations. *Hum Mutat*. 2014;35(9):E2403–E2412. doi:10.1002/humu.22619.
- [96] Ando Y, Ueda M. Novel methods for detecting amyloidogenic proteins in transthyretin related amyloidosis. *Front Biosci*. 2008;13(14):5548–5558. doi:10.2741/3098.
- [97] He S, Jin Y, Tian Z, et al. Establishment of an induced pluripotent stem cell line PUMCHI004-a from a hereditary transthyretin amyloid cardiomyopathy patient with transthyretin (TTR) p.Asp38Asn mutation. *Stem Cell Res*. 2020;49:102022. doi:10.1016/j.scr.2020.102022.
- [98] Aono Y, Hamatani Y, Katoh N, et al. Late-onset hereditary ATTR amyloidosis with a novel p.P63S (P43S) Transthyretin variant. *Intern Med*. 2021;60(4):557–561. doi:10.2169/internalmedicine.5615-20.
- [99] Groenning M, Campos RI, Fagerberg C, et al. Thermodynamic stability and denaturation kinetics of a benign natural transthyretin mutant identified in a danish kindred. *Amyloid*. 2011;18(2):35–46. doi:10.3109/13506129.2011.560215.
- [100] Cuddy SAM, Dorbala S, Falk RH. Complexities and pitfalls in cardiac amyloidosis. *Circulation*. 2020;142(4):409–415. doi:10.1161/circulationaha.120.046680.
- [101] Chen Z, Koh JS, Saini M, et al. Hereditary transthyretin amyloidosis—clinical and genetic characteristics of a multiracial South-East asian cohort in Singapore. *J Neuromuscul Dis*. 2021;8(4):723–733. doi:10.3233/JND-210656.
- [102] Reznik EV, Nguyen TL, Borisovskaya SV, et al. A clinical case of the hereditary transthyretin amyloidosis. *Russ Arch Intern Med*. 2021;11(3):229–240. doi:10.20514/2226-6704-2021-11-3-229-240.
- [103] Sant’Anna R, Almeida MR, Varejão N, et al. Cavity filling mutations at the thyroxine-binding site dramatically increase transthyretin stability and prevent its aggregation. *Sci Rep*. 2017;7(1):44709. doi:10.1038/srep44709.
- [104] Raivio VE, Jonasson J, Myllykangas L, et al. A novel transthyretin Lys70Glu (p.Lys90Glu) mutation presenting with vitreous amyloidosis and carpal tunnel syndrome. *Amyloid*. 2016;23(1):46–50. doi:10.3109/13506129.2015.1126574.
- [105] Bergström J, Patrosso MC, Colussi G, et al. A novel type of familial transthyretin amyloidosis, ATTR Asn124Ser, with co-localization of  $\kappa$  light chains. *Amyloid*. 2007;14(2):141–145. doi:10.1080/13506120701259895.
- [106] Choi K, Seok JM, Kim BJ, et al. Characteristics of South Korean patients with hereditary transthyretin amyloidosis. *J Clin Neurol*. 2018;14(4):537–541. doi:10.3988/jcn.2018.14.4.537.
- [107] Strahler JR, Rosenblum BB, Hanash SM. Identification and characterization of a human transthyretin variant. *Biochem Biophys Res Commun*. 1987;148(1):471–477. doi:10.1016/0006-291X(87)91135-1.
- [108] Lavigne Moreira C, Marques VD, Lourenço CM, et al. Transthyretin Asp38Tyr: a new mutation associated to a late onset neuropathy. *J Peripher Nerv Syst*. 2015;20(1):60–62. doi:10.1111/jns.12112.
- [109] Lavigne-Moreira C, Marques VD, Gonçalves MVM, et al. The genetic heterogeneity of hereditary transthyretin amyloidosis in a sample of the Brazilian population. *J Peripher Nerv Syst*. 2018;23(2):134–137. doi:10.1111/jns.12259.
- [110] Patel JK, Rosen AM, Chamberlin A, et al. Three newly recognized likely pathogenic gene variants associated with hereditary transthyretin amyloidosis. *Neurol Ther*. 2022;11(4):1595–1607. doi:10.1007/s40120-022-00385-1.
- [111] Thimm A, Oubari S, Hoffmann J, et al. A novel TTR mutation (p.Ala65Val) underlying late-onset hereditary transthyretin (ATTRv) amyloidosis with mixed cardiac and neuropathic phenotype: a case report. *BMC Neurol*. 2022;22(1):469. doi:10.1186/S12883-022-02952-3/FIGURES/4.
- [112] Ikeda K, Yamamoto D, Usui K, et al. A case of transthyretin variant amyloidosis with a TTR A97D (p.A117D) Mutation manifesting remarkable asymmetric neuropathy. *Intern Med*. 2022;62(15):2261–2266. Published online doi:10.2169/internalmedicine.0798-22.

- [113] Jiang M, Wang M, Tao Z, et al. Biochemical and biophysical properties of an unreported T96R mutation causing transthyretin cardiac amyloidosis. *Amyloid*. 2022;30(2):188–198. doi:10.1080/13506129.2022.2142109.
- [114] Ma Q, Wang M, Huang Y, et al. Identification of a novel transthyretin mutation D39Y in a cardiac amyloidosis patient and its biochemical characterizations. *Front Cardiovasc Med*. 2023;10:1091183. doi:10.3389/FCVM.2023.1091183.
- [115] Lyng CS, Gude E, Hodt A, et al. First Norwegian case of hereditary ATTR amyloidosis with a novel transthyretin variant. *Scand Cardiovasc J*. 2023;57(1):2174269. doi:10.1080/14017431.2023.2174269.
- [116] Waddington-Cruz M, Ackermann EJ, Polydefkis M, et al. Hereditary transthyretin amyloidosis: baseline characteristics of patients in the NEURO-TTR trial. *Amyloid*. 2018;25(3):180–188. doi:10.1080/13506129.2018.1503593.
- [117] Neculae G, Adam R, Beyer R, et al. Novel transthyretin variant linked to cardiac amyloidosis in the Romanian population. *Arch Cardiovasc Dis*. 2024;117(1):S38–S39. doi:10.1016/j.acvd.2023.10.068.
- [118] Stenson PD, Mort M, Ball EV, et al. The human gene mutation database (HGMD®): optimizing its use in a clinical diagnostic or research setting. *Hum Genet*. 2020;139(10):1197–1207. doi:10.1007/S00439-020-02199-3/FIGURES/5.
- [119] Landrum MJ, Lee JM, Riley GR, et al. ClinVar: public archive of relationships among sequence variation and human phenotype. *Nucleic Acids Res*. 2014;42(Database issue):D980–D985. doi:10.1093/NAR/GKT1113.
- [120] Uemichi T, Liepnieks JJ, Benson MD. A trinucleotide deletion in the transthyretin gene ( $\Delta V122$ ) in a kindred with familial amyloidotic polyneuropathy. *Neurology*. 1997;48(6):1667–1670. doi:10.1212/WNL.48.6.1667.
- [121] Klimtchuk ES, Prokaeva T, Frame NM, et al. Unusual duplication mutation in a surface loop of human transthyretin leads to an aggressive drug-resistant amyloid disease. *Proc Natl Acad Sci U S A*. 2018;115(28):E6428–E6436. doi:10.1073/pnas.1802977115.
- [122] Waddington-Cruz M, Ando Y, Amass L, et al. Feasibility of assessing progression of transthyretin amyloid polyneuropathy using nerve conduction studies: findings from the transthyretin amyloidosis outcomes survey (THAOS). *J Peripher Nerv Syst*. 2021;26(2):160–166. doi:10.1111/JNS.12444.
- [123] Sharp N. Mutations matter even if proteins stay the same. *Nature*. 2022;606(7915):657–659. doi:10.1038/d41586-022-01091-6.
- [124] Skare J, Jones LA, Myles N, et al. Two transthyretin mutations (glu42gly, his90asn) in an Italian family with amyloidosis. *Clin Genet*. 1994;45(6):281–284. doi:10.1111/J.1399-0004.1994.TB04030.X.
- [125] da Silva-Batista JA, Marques W, Oliveira MTdJS, et al. Presence of val30Met and val122ile mutations in a patient with hereditary amyloidosis. *J Hum Genet*. 2020;65(8):711–713. doi:10.1038/S10038-020-0749-3.
- [126] Lim A, Prokaeva T, Connors LH, et al. Identification of a novel transthyretin Thr59Lys/Arg104His. A case of compound heterozygosity in a Chinese patient diagnosed with familial transthyretin amyloidosis. *Amyloid*. 2002;9(2):134–140. doi:10.3109/13506120208995246.
- [127] Jacobson DR, Buxbaum JN. A double-variant transthyretin allele (SER 6, ILE 33) in the Israeli patient “SKO” with familial amyloidotic polyneuropathy. *Hum Mutat*. 1994;3(3):254–260. doi:10.1002/HUMU.1380030313.
- [128] Saraiva MJM. Transthyretin mutations in hyperthyroxinemia and amyloid diseases. *Hum Mutat*. 2001;17(6):493–503. doi:10.1002/HUMU.1132.
- [129] González-Duarte A, Cárdenas-Soto K, Bañuelos CE, et al. Amyloidosis due to TTR mutations in Mexico with 4 distinct genotypes in the index cases. *Orphanet J Rare Dis*. 2018;13(1):107. doi:10.1186/S13023-018-0801-Y/FIGURES/2.
- [130] Serpell LC, Goldsteins G, Dacklin I, et al. The “edge strand” hypothesis: prediction and test of a mutational “hot-spot” on the transthyretin molecule associated with FAP amyloidogenesis. *Amyloid*. 1996;3(2):75–85. doi:10.3109/13506129609014359.
- [131] Saraiva MJM. Transthyretin mutations in health and disease. *Hum Mutat*. 1995;5(3):191–196. doi:10.1002/humu.1380050302.
- [132] Salvi F, Pastorelli F, Plasmati R, et al. Early onset aggressive hereditary amyloidosis: report of an Italian family with TTR Arg47 mutation. *Neurol Sci*. 2005;26(2):140–142. doi:10.1007/s10072-005-0449-y.
- [133] Mangione PP, Porcari R, Gillmore JD, et al. Proteolytic cleavage of Ser52Pro variant transthyretin triggers its amyloid fibrillogenesis. *Proc Natl Acad Sci U S A*. 2014;111(4):1539–1544. doi:10.1073/pnas.1317488111.
- [134] Kim HS, Kim S-M, Kang S-W, et al. An aggressive form of familial amyloid polyneuropathy caused by a Glu54Gly mutation in the transthyretin gene. *Eur J Neurol*. 2005;12(8):657–659. doi:10.1111/j.1468-1331.2005.01005.x.
- [135] Togashi S, Watanabe H, Nagasaka T, et al. An aggressive familial amyloidotic polyneuropathy caused by a new variant transthyretin lys 54. *Neurology*. 1999;53(3):637–639. doi:10.1212/wnl.53.3.637.
- [136] Jacobson DR, McFarlin DE, Kane I, et al. Transthyretin Pro55, a variant associated with early-onset, aggressive, diffuse amyloidosis with cardiac and neurologic involvement. *Hum Genet*. 1992;89(3):353–356. doi:10.1007/BF00220559.
- [137] Gardini S, Cheli S, Baroni S, et al. On nature’s strategy for assigning genetic code multiplicity. Dupuy D, ed. *PLoS ONE*. 2016;11(2):e0148174. doi:10.1371/journal.pone.0148174.
- [138] Ueno S, Uemichi T, Yorifuji S, et al. A novel variant of transthyretin (Tyr114 to cys) deduced from the nucleotide sequences of gene fragments from familial amyloidotic polyneuropathy in Japanese sibling cases. *Biochem Biophys Res Commun*. 1990;169(1):143–147. doi:10.1016/0006-291X(90)91445-X.
- [139] Nakase T, Yamashita T, Matsuo Y, et al. Hereditary ATTR amyloidosis with cardiomyopathy caused by the novel variant transthyretin Y114S (p.Y134S). *Intern Med*. 2019;58(18):2695–2698. doi:10.2169/internalmedicine.2456-18.
- [140] Murakami T, Tachibana S, Endo Y, et al. Familial carpal tunnel syndrome due to amyloidogenic transthyretin his 114 variant. *Neurology*. 1994;44(2):315–318. doi:10.1212/wnl.44.2.315.
- [141] Janunger T, Anan I, Holmgren G, et al. Heart failure caused by a novel amyloidogenic mutation of the

- transthyretin gene: ATTR Ala45Ser. *Amyloid*. 2000;7(2):137–140. doi:10.3109/13506120009146252.
- [142] Saraiva MJ, Almeida MdR, Sherman W, et al. A new transthyretin mutation associated with amyloid cardiomyopathy. *Am J Hum Genet*. 1992;50(5):1027–1030.
- [143] Klaassen SHC, Lemmink HH, Bijzet J, et al. Late onset cardiomyopathy as presenting sign of ATTR A45G amyloidosis caused by a novel TTR mutation (p.A65G). *Cardiovasc Pathol*. 2017;29:19–22. doi:10.1016/j.carpath.2017.04.002.
- [144] Misumi Y, Doki T, Ueda M, et al. Myopathic phenotype of familial amyloid polyneuropathy with a rare transthyretin variant: ATTR Ala45Asp. *Amyloid*. 2014;21(3):216–217. doi:10.3109/13506129.2014.932277.
- [145] Murakami T, Maeda S, Yi S, et al. A novel transthyretin mutation associated with familial amyloidotic polyneuropathy. *Biochem Biophys Res Commun*. 1992;182(2):520–526. doi:10.1016/0006-291X(92)91763-G.
- [146] Ferlini A, Patrosso MC, Repetto M, et al. A new mutation (TTR ala-47) in the transthyretin gene associated with hereditary amyloidosis. *Hum Mutat*. 1994;4(1):61–64. doi:10.1002/humu.1380040110.
- [147] Pelo E, Da Prato L, Ciaccheri M, et al. Familial amyloid polyneuropathy with genetic anticipation associated to a gly47glu transthyretin variant in an Italian kindred. *Amyloid*. 2002;9(1):35–41. doi:10.3109/13506120209072443.
- [148] Booth DR, Soutar AK, Hawkins PN, et al. Three new amyloidogenic transthyretin gene mutations: advantages of direct sequencing. In: kisikevsky R, Benson MD, Frangione B, Gauldie J, Muckle TJ, Young ID, eds. *Amyloid and amyloidosis 1993*. 1st ed. Kingston (ON): Parthenon Publishing Group Ltd; 1994:456–458.
- [149] Ando Y, Coelho T, Berk JL, et al. Guideline of transthyretin-related hereditary amyloidosis for clinicians. *Orphanet J Rare Dis*. 2013;8(1):31. doi:10.1186/1750-1172-8-31.
- [150] Lemos C, Coelho T, Alves-Ferreira M, et al. Overcoming artefact: Anticipation in 284 portuguese kindreds with familial amyloid polyneuropathy (FAP) ATTRV30M. *J Neurol Neurosurg Psychiatry*. 2014;85(3):326–330. doi:10.1136/jnnp-2013-305383.
- [151] Ueda M, Yamashita T, Misumi Y, et al. Origin of sporadic late-onset hereditary ATTR Val30Met amyloidosis in Japan. *Amyloid*. 2018;25(3):143–147. doi:10.1080/13506129.2018.1531842.
- [152] Hellman U, Suhr O. Regional differences and similarities of FAP in Sweden. *Amyloid*. 2012;19 (sup1). 53–54.
- [153] Koike H, Misu K-I, Ikeda S-I, et al. Type I (transthyretin Met30) familial amyloid polyneuropathy in Japan: early- vs late-onset form. *Arch Neurol*. 2002;59(11):1771–1776. doi:10.1001/archneur.59.11.1771.
- [154] Ihse E, Ybo A, Suhr OB, et al. Amyloid fibril composition is related to the phenotype of hereditary transthyretin V30M amyloidosis. *J Pathol*. 2008;216(2):253–261. doi:10.1002/PATH.2411.
- [155] Suhr OB, Lundgren E, Westermark P. One mutation, two distinct disease variants: unravelling the impact of transthyretin amyloid fibril composition. *J Intern Med*. 2017;281(4):337–347. doi:10.1111/joim.12585.
- [156] Koike H, Ando Y, Ueda M, et al. Distinct characteristics of amyloid deposits in early- and late-onset transthyretin Val30Met familial amyloid polyneuropathy. *J Neurol Sci*. 2009;287(1-2):178–184. doi:10.1016/J.JNS.2009.07.028.
- [157] Keppel SC, Brannagan TH, Helmke S, et al. Early-Onset of transthyretin amyloidosis in a young Afro-Caribbean woman with Thr60Ala mutation. *JACC Case Rep*. 2020;2(13):2063–2067. doi:10.1016/j.jaccas.2020.08.030.
- [158] Kotani N, Hattori T, Yamagata S, et al. Transthyretin Thr60Ala appalachian-type mutation in a Japanese family with familial amyloidotic polyneuropathy. *Amyloid*. 2002;9(1):31–34. doi:10.3109/13506120209072442.
- [159] Soares ML, Coelho T, Sousa A, et al. Susceptibility and modifier genes in portuguese transthyretin V30M amyloid polyneuropathy: complexity in a single-gene disease. *Hum Mol Genet*. 2005;14(4):543–553. doi:10.1093/hmg/ddi051.
- [160] Santos D, Coelho T, Alves-Ferreira M, et al. Variants in RBP4 and AR genes modulate age at onset in familial amyloid polyneuropathy (FAP ATTRV30M). *Eur J Hum Genet*. 2016;24(5):756–760. doi:10.1038/ejhg.2015.180.
- [161] Olsson M, Hellman U, Planté-Bordeneuve V, et al. Mitochondrial haplogroup is associated with the phenotype of familial amyloidosis with polyneuropathy in Swedish and French patients. *Clin Genet*. 2009;75(2):163–168. doi:10.1111/J.1399-0004.2008.01097.X.
- [162] Alves-Ferreira M, Coelho T, Santos D, et al. A trans-acting factor may modify age at onset in familial amyloid polyneuropathy ATTRV30M in Portugal. *Mol Neurobiol*. 2018;55(5):3676–3683. doi:10.1007/s12035-017-0593-4.
- [163] Polimanti R, Di Girolamo M, Manfellotto D, et al. In silico analysis of TTR gene (coding and non-coding regions, and interactive network) and its implications in transthyretin-related amyloidosis. *Amyloid*. 2014;21(3):154–162. doi:10.3109/13506129.2014.900487.
- [164] Iorio A, De Angelis F, Di Girolamo M, et al. Most recent common ancestor of TTR Val30Met mutation in Italian population and its potential role in genotype-phenotype correlation. *Amyloid*. 2015;22(2):73–78. doi:10.3109/13506129.2014.994597.
- [165] Polimanti R, Di Girolamo M, Manfellotto D, et al. Functional variation of the transthyretin gene among human populations and its correlation with amyloidosis phenotypes. *Amyloid*. 2013;20(4):256–262. doi:10.3109/13506129.2013.844689.
- [166] Iorio A, De Lillo A, De Angelis F, et al. Non-coding variants contribute to the clinical heterogeneity of TTR amyloidosis. *Eur J Hum Genet*. 2017;25(9):1055–1060. doi:10.1038/ejhg.2017.95.
- [167] Iorio A, De Angelis F, Di Girolamo M, et al. Population diversity of the genetically determined TTR expression in human tissues and its implications in TTR amyloidosis. *BMC Genomics*. 2017;18(1):254. doi:10.1186/s12864-017-3646-1.
- [168] Polimanti R, Nuñez Y, Gelernter J. Increased risk of multiple outpatient surgeries in African-American carriers of transthyretin Val122Ile mutation is modulated by non-coding variants. *J Clin Med*. 2019;8(2):269. doi:10.3390/jcm8020269.
- [169] Sikora JL, Logue MW, Chan GG, et al. Genetic variation of the transthyretin gene in wild-type transthyretin amyloidosis (ATTRwt). *Hum Genet*. 2015;134(1):111–121. doi:10.1007/s00439-014-1499-0.

- [170] Quintas A, Vaz DC, Cardoso I, et al. Tetramer dissociation and monomer partial unfolding precedes protofibril formation in amyloidogenic transthyretin variants. *J Biol Chem.* 2001;276(29):27207–27213. doi:10.1074/jbc.M101024200.
- [171] Hörnberg A, Eneqvist T, Olofsson A, et al. A comparative analysis of 23 structures of the amyloidogenic protein transthyretin. *J Mol Biol.* 2000;302(3):649–669. doi:10.1006/jmbi.2000.4078.
- [172] Palaninathan SK. Nearly 200 X-Ray crystal structures of transthyretin: what do they tell us about this protein and the design of drugs for TTR amyloidosis? *Curr Med Chem.* 2012;19(15):2324–2342. doi:10.2174/092986712800269335.
- [173] Brito RMM, Damas AM, Saraiva MJ. Amyloid formation by transthyretin: from protein stability to protein aggregation. *Curr Med Chem Endocr Metab Agents.* 2003;3(4):349–360. doi:10.2174/1568013033483230.
- [174] Palaninathan SK, Mohamedmohaideen NN, Snee WC, et al. Structural insight into pH-induced conformational changes within the native human transthyretin tetramer. *J Mol Biol.* 2008;382(5):1157–1167. doi:10.1016/j.jmb.2008.07.029.
- [175] Dasari AKR, Hung I, Michael B, et al. Structural characterization of cardiac ex vivo transthyretin amyloid: insight into the transthyretin misfolding pathway in vivo. *Biochemistry.* 2020;59(19):1800–1803. doi:10.1021/acs.biochem.0c00091.
- [176] Schmidt M, Wiese S, Adak V, et al. Cryo-EM structure of a transthyretin-derived amyloid fibril from a patient with hereditary ATTR amyloidosis. *Nat Commun.* 2019;10(1):5008. doi:10.1038/s41467-019-13038-z.
- [177] Ferguson JA, Sun X, Dyson HJ, et al. Thermodynamic stability and aggregation kinetics of EF helix and EF loop variants of transthyretin. *Biochemistry.* 2021;60(10):756–764. doi:10.1021/acs.biochem.1c00073.
- [178] Yang M, Lei M, Bruschweiler R, et al. Initial conformational changes of human transthyretin under partially denaturing conditions. *Biophys J.* 2005;89(1):433–443. doi:10.1529/biophysj.105.059642.
- [179] Yang M, Yordanov B, Levy Y, et al. The sequence-dependent unfolding pathway plays a critical role in the amyloidogenicity of transthyretin. *Biochemistry.* 2006;45(39):11992–12002. doi:10.1021/bi0609927.
- [180] Rodrigues JR, Simões CJV, Silva CG, et al. Potentially amyloidogenic conformational intermediates populate the unfolding landscape of transthyretin: insights from molecular dynamics simulations. *Protein Sci.* 2010;19(2):202–219. doi:10.1002/pro.289.
- [181] Lai Z, Colón W, Kelly JW. The acid-mediated denaturation pathway of transthyretin yields a conformational intermediate that can self-assemble into amyloid. *Biochemistry.* 1996;35(20):6470–6482. doi:10.1021/bi952501g.
- [182] Olofsson A, Ippel JH, Wijmenga SS, et al. Probing solvent accessibility of transthyretin amyloid by solution NMR spectroscopy. *J Biol Chem.* 2004;279(7):5699–5707. doi:10.1074/jbc.M310605200.
- [183] Serag AA, Altenbach C, Gingery M, et al. Arrangement of subunits and ordering of  $\beta$ -strands in an amyloid sheet. *Nat Struct Biol.* 2002;9(10):734–739. doi:10.1038/nsb838.
- [184] Goldsteins G, Persson H, Andersson K, et al. Exposure of cryptic epitopes on transthyretin only in amyloid and in amyloidogenic mutants. *Proc Natl Acad Sci U S A.* 1999;96(6):3108–3113. doi:10.1073/pnas.96.6.3108.
- [185] Yee AW, Aldeghi M, Blakeley MP, et al. A molecular mechanism for transthyretin amyloidogenesis. *Nat Commun.* 2019;10(1):925. doi:10.1038/s41467-019-08609-z.
- [186] Wang Y-S, Huang C-H, Liou G-G, et al. A molecular basis for tetramer destabilization and aggregation of transthyretin Ala97Ser. *Protein Sci.* 2023;32(4):e4610. doi:10.1002/PRO.4610.
- [187] Dasari AKR, Arreola J, Michael B, et al. Disruption of the CD loop by enzymatic cleavage promotes the formation of toxic transthyretin oligomers through a common transthyretin misfolding pathway. *Biochemistry.* 2020;59(25):2319–2327. doi:10.1021/acs.biochem.0c00079.
- [188] Zhou S, Cheng J, Yang T, et al. Exploration of the misfolding mechanism of transthyretin monomer: insights from Hybrid-Resolution simulations and markov state model analysis. *Biomolecules.* 2019;9(12):889. doi:10.3390/biom9120889.
- [189] Lim KH, Dyson HJ, Kelly JW, et al. Localized structural fluctuations promote amyloidogenic conformations in transthyretin. *J Mol Biol.* 2013;425(6):977–988. doi:10.1016/j.jmb.2013.01.008.
- [190] Lim KH, Dasari AKR, Hung I, et al. Structural changes associated with transthyretin misfolding and amyloid formation revealed by solution and solid-State NMR. *Biochemistry.* 2016;55(13):1941–1944. doi:10.1021/acs.biochem.6b00164.
- [191] Armen RS, Alonso DOV, Daggett V. Anatomy of an amyloidogenic intermediate: conversion of  $\beta$ -sheet to  $\alpha$ -sheet structure in transthyretin at acidic pH. *Structure.* 2004;12(10):1847–1863. doi:10.1016/j.str.2004.08.005.
- [192] Steward RE, Armen RS, Daggett V. Different disease-causing mutations in transthyretin trigger the same conformational conversion. *Protein Eng Des Sel.* 2008;21(3):187–195. doi:10.1093/protein/gzm086.
- [193] Kelly JW. Alternative conformations of amyloidogenic proteins govern their behavior. *Curr Opin Struct Biol.* 1996;6(1):11–17. doi:10.1016/S0959-440X(96)80089-3.
- [194] Uversky VN, Segel DJ, Doniach S, et al. Association-induced folding of globular proteins. *Proc Natl Acad Sci U S A.* 1998;95(10):5480–5483. doi:10.1073/pnas.95.10.5480.
- [195] Terry CJ, Damas AM, Oliveira P, et al. Structure of Met30 variant of transthyretin and its amyloidogenic implications. *Embo J.* 1993;12(2):735–741. doi:10.1002/j.1460-2075.1993.tb05707.x.
- [196] Eneqvist T, Andersson K, Olofsson A, et al. The  $\beta$ -slip: a novel concept in transthyretin amyloidosis. *Mol Cell.* 2000;6(5):1207–1218. doi:10.1016/s1097-2765(00)00117-9.
- [197] Ferrão-Gonzales AO, Souto SO, Silva JL, et al. The pre-aggregated state of an amyloidogenic protein: Hydrostatic pressure converts native transthyretin into the amyloidogenic state. *Proc Natl Acad Sci U S A.* 2000;97(12):6445–6450. doi:10.1073/pnas.97.12.6445.
- [198] Schormann N, Murrell JR, Benson MD. Tertiary structures of amyloidogenic and non-amyloidogenic transthyretin variants: new model for amyloid fibril formation. *Amyloid.* 1998;5(3):175–187. doi:10.3109/13506129809003843.
- [199] Olofsson A, Ippel HJ, Baranov V, et al. Capture of a dimeric intermediate during transthyretin amyloid forma-

- tion. *J Biol Chem.* 2001;276(43):39592–39599. doi:10.1074/jbc.M103599200.
- [200] Serag AA, Altenbach C, Gingery M, et al. Identification of a subunit interface in transthyretin amyloid fibrils: evidence for self-assembly from oligomeric building blocks. *Biochemistry.* 2001;40(31):9089–9096. doi:10.1021/bi010655s.
- [201] Lashuel HA, Lai Z, Kelly JW. Characterization of the transthyretin acid denaturation pathways by analytical ultracentrifugation: implications for wild-type, V30M, and L55P amyloid fibril formation. *Biochemistry.* 1998;37(51):17851–17864. doi:10.1021/BI981876+.
- [202] Nettleton EJ, Sunde M, Lai Z, et al. Protein subunit interactions and structural integrity of amyloidogenic transthyretins: evidence from electrospray mass spectrometry. *J Mol Biol.* 1998;281(3):553–564. doi:10.1006/jmbi.1998.1937.
- [203] Lindgren M, Sörgjerd K, Hammarström P. Detection and characterization of aggregates, prefibrillar amyloidogenic oligomers, and protofibrils using fluorescence spectroscopy. *Biophys J.* 2005;88(6):4200–4212. doi:10.1529/biophysj.104.049700.
- [204] Lindgren M, Hammarström P. Amyloid oligomers: spectroscopic characterization of amyloidogenic protein states. *Febs J.* 2010;277(6):1380–1388. doi:10.1111/j.1742-4658.2010.07571.x.
- [205] Inouye H, Domingues FS, Damas AM, et al. Analysis of x-ray diffraction patterns from amyloid of biopsied vitreous humor and kidney of transthyretin (TTR) Met30 familial amyloidotic polyneuropathy (FAP) patients: Axially arrayed TTR monomers constitute the protofilament. *Amyloid.* 1998;5(3):163–174. doi:10.3109/13506129809003842.
- [206] Saelices L, Nguyen BA, Chung K, et al. A pair of peptides inhibits seeding of the hormone transporter transthyretin into amyloid fibrils. *J Biol Chem.* 2019;294(15):6130–6141. doi:10.1074/jbc.RA118.005257.
- [207] Quintas A, Saraiva MJM, Brito RMM. The tetrameric protein transthyretin dissociates to a non-native monomer in solution. A novel model for amyloidogenesis. *J Biol Chem.* 1999;274(46):32943–32949. doi:10.1074/jbc.274.46.32943.
- [208] Foss TR, Wiseman RL, Kelly JW. The pathway by which the tetrameric protein transthyretin dissociates. *Biochemistry.* 2005;44(47):15525–15533. doi:10.1021/bi051608t.
- [209] Coelho T, Merlini G, Bulawa CE, et al. Mechanism of action and clinical application of tafamidis in hereditary transthyretin amyloidosis. *Neurol Ther.* 2016;5(1):1–25. doi:10.1007/s40120-016-0040-x.
- [210] Jesus C, Almeida Z, Vaz D, et al. A new folding kinetic mechanism for human transthyretin and the influence of the amyloidogenic V30M mutation. *Int J Mol Sci.* 2016;17(9):1428. doi:10.3390/ijms17091428.
- [211] Simões CJV, Almeida ZL, Costa D, et al. A novel bis-furan scaffold for transthyretin stabilization and amyloid inhibition. *Eur J Med Chem.* 2016;121:823–840. doi:10.1016/j.ejmech.2016.02.074.
- [212] Simões CJV, Almeida ZL, Cardoso AL, et al. Lead optimization of resilient next-generation transthyretin stabilizers for multiple target-product profiles: approaching the CNS. *Amyloid.* 2019;26(sup1):77–78. doi:10.1080/13506129.2019.1583195.
- [213] Ferreira E, Almeida ZL, Cruz PF, et al. Searching for the best transthyretin aggregation protocol to study amyloid fibril disruption. *Int J Mol Sci.* 2022;23(1):391. doi:10.3390/ijms23010391.
- [214] Almeida ZL, Brito RMM. Amyloid disassembly: what can We learn from chaperones? *Biomedicines.* 2022;10(12):3276. doi:10.3390/biomedicines10123276.
- [215] Cardoso I, Goldsbury CS, Müller SA, et al. Transthyretin fibrillogenesis entails the assembly of monomers: a molecular model for in vitro assembled transthyretin amyloid-like fibrils. *J Mol Biol.* 2002;317(5):683–695. doi:10.1006/jmbi.2002.5441.
- [216] Sant’Anna R, Braga C, Varejão N, et al. The importance of a gatekeeper residue on the aggregation of transthyretin implications for transthyretin-related amyloidoses. *J Biol Chem.* 2014;289(41):28324–28337. doi:10.1074/jbc.M114.563981.
- [217] Faria TQ, Almeida ZL, Cruz PF, et al. A look into amyloid formation by transthyretin: Aggregation pathway and a novel kinetic model. *Phys Chem Chem Phys.* 2015;17(11):7255–7263. doi:10.1039/c4cp04549a.
- [218] Jarvis JA, Craik DJ, Wilce MCJ. X-ray-diffraction studies of fibrils formed from peptide fragments of transthyretin. *Biochem Biophys Res Commun.* 1993;192(3):991–998. doi:10.1006/bbrc.1993.1514.
- [219] Dirix C, Meersman F, MacPhee CE, et al. High hydrostatic pressure dissociates early aggregates of TTR 105-115, but not the mature amyloid fibrils. *J Mol Biol.* 2005;347(5):903–909. doi:10.1016/j.jmb.2005.01.073.
- [220] Gustavsson Å, Engström U, Westermark P. Normal transthyretin and synthetic transthyretin fragments from amyloid-like fibrils in vitro. *Biochem Biophys Res Commun.* 1991;175(3):1159–1164. doi:10.1016/0006-291X(91)91687-8.
- [221] Bergström J, Engström U, Yamashita T, et al. Surface exposed epitopes and structural heterogeneity of in vivo formed transthyretin amyloid fibrils. *Biochem Biophys Res Commun.* 2006;348(2):532–539. doi:10.1016/j.bbrc.2006.07.140.
- [222] Colon W, Kelly JW. Partial denaturation of transthyretin is sufficient for amyloid fibril formation in vitro. *Biochemistry.* 1992;31(36):8654–8660. doi:10.1021/bi00151a036.
- [223] Groenning M, Campos RI, Hirschberg D, et al. Considerably unfolded transthyretin monomers precede and exchange with dynamically structured amyloid protofibrils. *Sci Rep.* 2015;5(1):11443. doi:10.1038/srep11443.
- [224] Pires RH, Karsai Á, Saraiva MJ, et al. Distinct annular oligomers captured along the assembly and disassembly pathways of transthyretin amyloid protofibrils. Muller DJ, ed. *PLoS One.* 2012;7(9):e44992. doi:10.1371/journal.pone.0044992.
- [225] Frangolho A, Correia BE, Vaz DC, et al. Oligomerization profile of human transthyretin variants with distinct amyloidogenicity. *Molecules.* 2020;25(23):5698. doi:10.3390/molecules25235698.
- [226] Dolado I, Nieto J, Saraiva MJM, et al. Kinetic assay for high-throughput screening of in vitro transthyretin amyloid fibrillogenesis inhibitors. *J Comb Chem.* 2005;7(2):246–252. doi:10.1021/cc049849s.
- [227] Saelices L, Chung K, Lee JH, et al. Amyloid seeding of transthyretin by ex vivo cardiac fibrils and its inhibi-

- tion. Proc Natl Acad Sci U S A. 2018;115(29):E6741–E6750. doi:[10.1073/pnas.1805131115](https://doi.org/10.1073/pnas.1805131115).
- [228] Foguel D, Suarez MC, Ferrão-Gonzales AD, et al. Dissociation of amyloid fibrils of  $\alpha$ -synuclein and transthyretin by pressure reveals their reversible nature and the formation of water-excluded cavities. Proc Natl Acad Sci U S A. 2003;100(17):9831–9836. doi:[10.1073/pnas.1734009100](https://doi.org/10.1073/pnas.1734009100).
- [229] Cardoso I, Merlini G, Saraiva MJ. 4'-Iodo-4'-deoxydoxorubicin and tetracyclines disrupt transthyretin amyloid fibrils in vitro producing noncytotoxic species: Screening for TTR fibril disrupters. Faseb J. 2003;17(8):803–809. doi:[10.1096/fj.02-0764com](https://doi.org/10.1096/fj.02-0764com).
- [230] Bonifácio MJ, Sakaki Y, Saraiva MJ. "In vitro" amyloid fibril formation from transthyretin: the influence of ions and the amyloidogenicity of TTR variants. Biochim Biophys Acta. 1996;1316(1):35–42. doi:[10.1016/0925-4439\(96\)00014-2](https://doi.org/10.1016/0925-4439(96)00014-2).
- [231] Lundberg E, Olofsson A, Westermark GT, et al. Stability and fibril formation properties of human and fish transthyretin, and of the *Escherichia coli* transthyretin-related protein. Febs J. 2009;276(7):1999–2011. doi:[10.1111/j.1742-4658.2009.06936.x](https://doi.org/10.1111/j.1742-4658.2009.06936.x).
- [232] Marcoux J, Mangione PP, Porcari R, et al. A novel mechano-enzymatic cleavage mechanism underlies transthyretin amyloidogenesis. EMBO Mol Med. 2015;7(10):1337–1349. doi:[10.15252/emmm.201505357](https://doi.org/10.15252/emmm.201505357).
- [233] Mangione PP, Verona G, Corazza A, et al. Plasminogen activation triggers transthyretin amyloidogenesis in vitro. J Biol Chem. 2018;293(37):14192–14199. doi:[10.1074/jbc.RA118.003990](https://doi.org/10.1074/jbc.RA118.003990).
- [234] Saelices L, Johnson LM, Liang WY, et al. Uncovering the mechanism of aggregation of human transthyretin. J Biol Chem. 2015;290(48):28932–28943. doi:[10.1074/jbc.M115.659912](https://doi.org/10.1074/jbc.M115.659912).
- [235] Dasari AKR, Yi S, Coats MF, et al. Toxic misfolded transthyretin oligomers with different molecular conformations formed through distinct oligomerization pathways. Biochemistry. 2022;61(21):2358–2365. doi:[10.1021/acs.biochem.2c00390](https://doi.org/10.1021/acs.biochem.2c00390).
- [236] Moreira L, Beirão JM, Beirão I, et al. Oligomeric TTR V30M aggregates compromise cell viability, erythropoietin gene expression and promoter activity in the human hepatoma cell line Hep3B. Amyloid. 2015;22(2):93–99. doi:[10.3109/13506129.2015.1007497](https://doi.org/10.3109/13506129.2015.1007497).